Hydrogen for X-group exchange in CHX (X = Cl, Br, I , OMe, and NMe) by monomeric [1,2,4-(Me3C)3C5H2]2CeH: experimental and computational support for a carbenoid mechanism

Evan L. Werkema, Richard A. Andersen, Ahmed Yahia, Laurent Maron, Odile Eisenstein

Hydrogen for X-group exchange in CH_3X, X = Cl, Br, I, OMe and NMe_2 by Monomeric $[1,2,4\text{-}(Me_3C)_3C_5H_2]_2CeH$: Experimental and Computational Support for a Carbenoid Mechanism

Evan L. Werkema[a], Richard A. Andersen*[a], Ahmed Yahia[b], Laurent Maron*[b] and Odile Eisenstein*[c]

a) Department of Chemistry, University of California, Berkeley, California 94720-1460, b) Université de Toulouse, INSA, UPS, LPCNO, 135 avenue de Rangueil, 31077 Toulouse, France, and CNRS, 31077 Toulouse, France, c) Université Montpellier 2, Institut Charles Gerhardt, UMR 5253 CNRS-UM2-ENSCM-UM1, Place E. Bataillon, 34095 Montpellier France, and CNRS, Institut Charles Gerhardt, France,

Abstract

The reaction between $[1,2,4\text{-}(Me_3C)_3C_5H_2]_2CeH$, referred to as Cp'_2CeH, and CH_3X where X is Cl, Br, I, OMe and NMe_2, are described. The reactions fall into three distinct classes. Class a, where X = Cl, Br and I rapidly form Cp'_2CeX and CH_4 without formation of identifiable intermediates in the ^1H NMR spectra. Class b, where X = OMe proceeds rapidly to $Cp'_2Ce(\eta^2\text{-}CH_2OMe)$ and H_2 and then to Cp'_2CeOMe and CH_4. The methoxymethyl derivative is sufficiently stable to be isolated and characterized and it is rapidly converted to Cp'_2CeOMe in presence of BPh_3. Class c, where X = NMe_2 does not result in formation of Cp'_2CeNMe_2, but deuterium labeling experiments show that H for D exchange occurs in NMe_3. Density functional calculations DFT(B3PW91) on the reaction of $(C_5H_5)_2CeH$, referred to as Cp_2CeH,

and CH_3X show that the barrier for α-CH activation, resulting in formation of $Cp_2Ce(\eta^2\text{-}CH_2X)$, proceeds with a relatively low activation barrier ($\Delta G^{\ddagger}$) but the subsequent ejection of CH_2 and trapping by H_2 has a higher barrier; the height of the second barrier lies in the order F, Cl, Br, I < OMe << NMe_2, consistent with the experimental studies. The DFT calculations also show that the two-step reaction, which proceeds through a carbenoid intermediate, has a lower barrier than a direct one-step σ bond metathesis mechanism. The reaction of Cp_2CeCH_2OMe and BPh_3 is calculated to be a low barrier process and the ylide, $CH_2^{(+)}BPh_3^{(-)}$, is a transition state and not an intermediate.

Introduction

The reaction between CH_3F and $[1,2,4\text{-}(Me_3C)_3C_5H_2]_2CeH$, referred to as Cp'_2CeH in this article, to give CH_4 and Cp'_2CeF has been described recently.[1] The net reaction involves a Ce-H for C-F exchange that is strongly exoergic; ΔG for the model system $(C_5H_5)_2CeH$ and CH_3F in gas phase was calculated by DFT methods to be -77 kcal mol^{-1}. Although the C-F BDE in CH_3F is 108 kcal mol^{-1},[2] the Ce-F bond is considerably stronger, the average Ce-F bond enthalpy of $CeF_3(g)$ is 153 kcal mol^{-1},[3] and the net reaction is exothermic. The mechanism of the exchange reaction does not proceed by a σ-bond metathesis transition state as shown by calculational and experimental studies. The calculated activation energy in the model system for a σ-bond metathesis is 31 kcal mol^{-1} relative to the reactants, too high for a reaction that is rapid and irreversible at 20°C. The high energy barrier originates from the methyl group occupying the β-site in the 4c-4e metathesis transition state **I**, resulting in a five coordinate carbon atom that is high in energy. Calculations showed that an activation energy of only 18 kcal mol^{-1} was required when an α-CH activation occurs in

transition state **II**. In transition state **II**, the product, CH_4, was derived from trapping of the CH_2 fragment by dihydrogen. Thus the lower activation energy pathway suggested by the calculation is a stepwise or indirect process that proceeds by way of carbenoid fragment **III**. The indirect α-CH activation pathway discovered in the calculational studies was supported by experimental studies, such as trapping the CH_2 fragment with cyclohexene. Accordingly, the carbenoid pathway for the reaction between CH_3F and Cp'_2CeH was placed on a firm foundation, but the question of generality was not addressed in the original article.

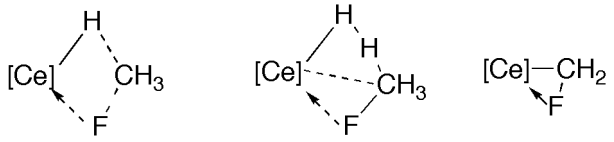

I **II** **III**

In this article, the results of the reaction between CH_3X, X = Cl, Br, I, OMe, NMe_2 and Cp'_2CeH are described from a calculational and experimental perspective with the general result that the carbenoid pathway is followed for these simple substituted methane derivatives.

Results

General Experimental Studies

The experimental methodology that was used in the earlier article is used in the present one.[1] The time evolution of the reaction between Cp'_2CeH and the MeX derivatives is followed by ^1H NMR spectroscopy in either C_6D_6 or C_6D_{12} at 20°C. Since the reactant and product metallocenes are paramagnetic, the Me_3C-resonances on the 1,2,4-$(Me_3C)_3C_5H_2$ rings are a convenient probe to assay the extent, relative rates, and cleanliness of the net reactions; the ring methyne-resonances are often not

observed. After the reactions are complete, hydrolysis (H_2O) and GCMS analysis of the hydrosylate is used to identify the organic products in each experiment. As described in the earlier article, the reactions between the metallacycle, [1,2,4-$(Me_3C)_3C_5H_2$] [$(Me_3C)_2C_5H_2C(CH_3)_2CH_2$]Ce, **1**, abbreviated Cp'[$(Me_3C)_2C_5H_2C(CH_3)_2CH_2$)Ce or simply as metallacycle, **1**, with the MeX derivatives are followed by ^{1}H NMR spectroscopy and the identity of the organic products is determined by GCMS after hydrolysis.

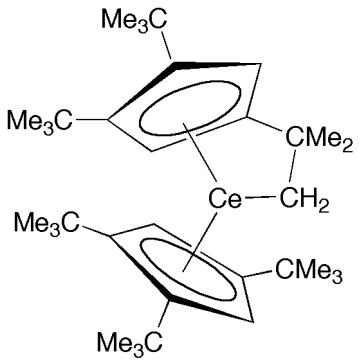

1

In the reactions of **1**, dihydrogen is not present and cannot serve as a trap for the methylene fragment and therefore intermediates may be observed in the ^{1}H NMR spectra. In addition, added trapping reagents that do not react with **1** may be employed. The cerium containing products Cp'$_2$CeX are prepared independently, isolated and characterized as outlined in the Experimental Section or in the text.

Reaction of Cp'$_2$CeH or metallacycle, 1, with CH_3X, X = Cl, Br, and I

The reaction between Cp'$_2$CeH and CH_3X, X = Cl, Br, and I, are rapid and clean at 20°C, as only resonances due to Cp'$_2$CeX and CH_4 are observed in the ^{1}H NMR spectrum, eq 1.

$$Cp'_2CeH + CH_3X \rightarrow Cp'_2CeX + CH_4 \qquad X = Cl, Br, I \qquad (1)$$

Thus, the net reactions of all of the methylhalides are similar. The reaction between the methylhalides and the metallacycle is slightly more complicated. The reaction with CH_3Cl is clean, since the resonances in the ^1H NMR spectrum due to metallacycle, **1**, in C_6D_{12} disappear within approximately 15 minutes and a new set of Me_3C-resonances, referred to as Q_{Cl}, appear at δ -1.36 and δ -8.54 in ratio of 2:1, in addition to resonances due to Cp'_2CeCl, and the metallocene. Over time, the resonances due to Q_{Cl} disappear and resonances due to Cp'_2CeCl increase in intensity. After approximatively three days, the conversion is complete; since the solubility of Cp'_2CeCl is low in these solvents, mass balance cannot be obtained by integration of the NMR spectrum. When the reaction is complete, hydrolysis of the mixture and analysis of the hydrolysate by GCMS shows the presence of Cp'H and Cp"H where Cp" represents the isomers of 1,2-(Me_3C)-4-(Me_2**Et**C)C_5H_3 as observed in the reaction with CH_3F.[1] Thus the net reaction between the metallacycle, **1**, with CH_3F and CH_3Cl give similar final products, but intermediate, Q_F, is not detected.[1] As in the reaction of CH_3F, a CH-bond of a Me_3C group in the Cp'-ring acts as a trap of the CH_2 fragment, eq 2.

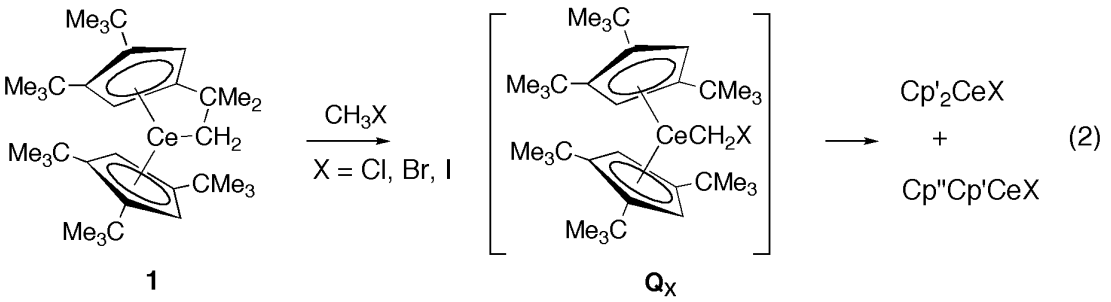

Since the final products in the case of CH_3F and CH_3Cl are similar, both reactions presumably follow similar mechanisms, *viz*, the generation of a carbenoid intermediate, Q_X, followed by ejection of CH_2 and trapping by H_2 in the case of

Cp'_2CeH or the CH bond of a Me_3C- group in the Cp'-ring when H_2 is absent. The only difference between the CH_3F and CH_3Cl reactions is that Q_{Cl} builds up in the latter reaction and Q_F does not.

The reaction of CH_3Br and CH_3I with the metallacycle, **1**, is similar to that of CH_3Cl, eq 2. In the case of CH_3Br, the resonances attributed to Q_{Br} appear at δ -1.36 and δ -8.16 in a ratio of 2:1. Exposure of the metallacycle, 1, to CD_3Br in toluene and examining the organic products, after hydrolysis, by GCMS shows the presence of Cp'H and Cp"H-d_2. This result shows that Q_{Br} eliminates CD_2, which is trapped by the Me_3C-groups on the Cp'-ring. No deuterium is detected in solvent toluene and therefore the intramolecular trapping of CD_2 is more efficient than is intermolecular trapping by the solvent CH bonds.

In the CH_3I reaction, two resonances in a 2:1 ratio due to Q_I at δ -1.3 and δ -7.8 appear within 10 minutes of mixing. After approximately 3 hours resonances due to Cp'_2CeI form and the ratio of Q_I: Cp'_2CeI is 6:1. After 5 days at 20°C, Q_I disappears and only those resonances due to Cp'_2CeI remain. In all three reactions, the resonances attributed to Q_X have similar chemical shifts which implies that the Me_3C-groups on the Cp'-rings are in a similar geometrical arrangement; a postulated structure is shown in eq 2 for all three intermediates. This deduction is developed in more detail in the next section.

Reaction of Cp'_2CeH and metallacycle, 1, with CH_3OMe.

Mixing Cp'_2CeH and CH_3OMe in C_6D_6 in an NMR tube results in disappearance of the resonances due to Cp'_2CeH within 15 minutes and appearance of two new sets of Me_3C-resonances at δ -1.11 and δ -10.9 (2:1), Q_{OMe}, and δ -2.38 and δ -4.43 (2:1), Q'_{OMe}. After two days at 20°C an additional set of resonances appears due

to Cp'_2CeOMe.[4] The ratio of Q_{OMe}: Q'_{OMe} : Cp'_2CeOMe is 40: 50: 1. Heating at 60°C for 27 days increases the quantity of Cp'_2CeOMe since the ratio is now 3:1:7, eq 3, which only shows the cerium containing compounds that are identified.

$$Cp'_2CeH + CH_3OMe \rightarrow Q_{OMe} \text{ and } Q'_{OMe} + H_2 \rightarrow Cp'_2CeOMe + CH_4 \quad (3)$$

The identity of Q_{OMe} is presumably similar to that of Q_X, X = Cl, Br, I since the pattern of the chemical shifts of the Me_3C-resonances is similar. The identity of Q'_{OMe}, remains unknown, though it might be a Me_2O adduct of either Q_{OMe} and Cp'_2CeH, since evaporation to dryness and dissolution in C_6D_6 results in resonances only due to Q_{OMe} and Cp'_2CeH.

The reaction of CH_3OMe with metallacycle, **1**, is rather more straightforward since mixing the two reactants results in appearance of resonances due to Q_{OMe} within 20 minutes at 20°C. Evaporation of the solution to dryness, dissolution in C_6D_{12} followed by heating the mixture to 60°C for a day, then cooling to 20°C and examining the ^1H NMR spectrum shows resonances due to Q_{OMe} and metallacycle, **1**, in a 11:1 ratio; heating to 60°C for three days does not alter the ratio of Q_{OMe}:**1** from 11:1. Thus, Q_{OMe} has an appreciable lifetime in absence of H_2 and should be isolable, see below. In addition, Q_{OMe} and the metallacycle are in equilibrium, eq 4.

$$\text{Metallacycle, } \mathbf{1} + CH_3OMe \rightleftharpoons Q_{OMe} \quad (4)$$

The equilibrium, illustrated by eq 4, is substantiated by exposing the perdeuterometallacycle, **1-d$_{53}$** to CH_3OMe in C_6D_{12}. The ^1H NMR spectrum shows resonances due to the $C(CD_{3-x}H_x)_3$ groups and Q_{OMe} after 30 minutes at 20°C. The relative amounts change little over two days. The ^2H NMR spectrum also shows

resonances due to the $C(CD_{3-x}H_x)_3$ groups forming over this period of time. Heating to 60°C for three days results in appearance of resonances due to Me_2O-d_1, which appear as a 1:1:1 pattern in the ^1H NMR spectrum at $\delta_H = 3.16$ and $J_{HD} = 1.2$ Hz. The ^1H NMR spectrum also shows resonances due to H for D exchange in the Me_3C groups on the Cp' rings. After three days at 60°C, the deuterium is preferentially located at the unique Me_3C group, but heating the mixture at 60°C for 81 days results in a ^1H NMR spectrum in which a single hydrogen atom is statistically distributed into the three Me_3C groups, see Experimental Section for details. The labeling study shows that insertion of the CH bond of CH_3OMe into the metallacycle Ce-C bond is rapid but elimination of CH_2DOMe is slow, which rationalizes why Q_{OMe} is an isolable compound.

On a synthetic scale, addition of an excess of dimethylether to a solution of Cp'_2CeH in pentane results in a color change from purple to red. Concentrating and cooling the solution gives red crystals of Cp'_2CeCH_2OMe in 37% yield. The methoxymethyl derivative turns deep purple on heating in a sealed tube at 135°C and then melts at 210-213°C. No molecular ion is observed in the mass spectrum but the fragment with highest m/e is $[M\text{-}CH_2OMe]^+$; a similar fragmentation pattern is observed for Cp'_2CeCH_2Ph, i.e., $[M\text{-}CH_2Ph]^+$.[5] The ^1H NMR spectrum of Cp'_2CeCH_2OMe at 20°C shows the Me_3C-resonances in a 1:2 ratio, though the resonance of area 2 is broadened, and the OMe resonance is a singlet; the methylene resonance and the ring-methyne resonances are not observed. The variable temperature ^1H NMR spectrum for the Me_3C-groups is shown as a δ vs T^{-1} plot in Figure 1. The methoxymethyl group resonance is a curve and therefore does not follow Curie law.

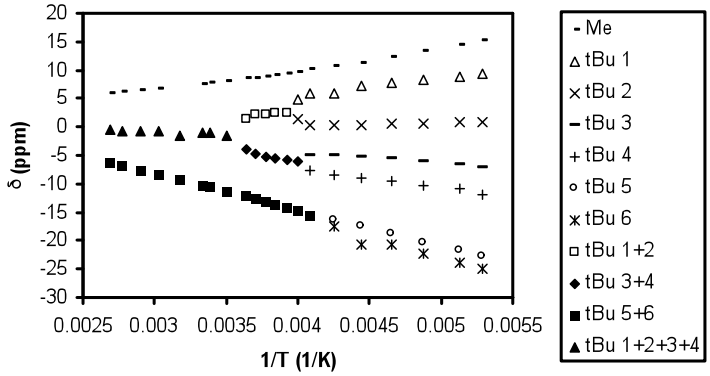

Figure 1. δ vs. 1/T plot for $Cp'_2CeCH_2OCH_3$ showing the Me_3C resonances on the Cp' rings and the OMe resonance.

The observation that all of the Me_3C-groups are chemically inequivalent at temperatures below about -30°C is rare in $Cp'_2M(X)(Y)$ metallocene derivatives. Generally, the two Cp'-rings are free to oscillate about their pseudo C_5 axes generating a molecule with averaged C_{2v} symmetry and the CMe_3 groups are observed in a 1:2 ratio. As the temperature is lowered the time averaged mirror plane and the C_2 axes are removed and the CMe_3 groups appear in a 1:1:1 ratio. The inequivalence of all six Me_3C-groups was observed in one metallocene, *viz.*, $Cp'_2UN(Me)C(Ph)C(Ph)$[6]. In Cp'_2CeCH_2OMe, the molecule can have averaged C_{2v} symmetry if the CH_2OMe is monodentate and C_s symmetry if bidentate, accounting for the 1:2 and 1:1:1 pattern, respectively. The inequivalence of all six CMe_3 groups means that the molecule has C_1 symmetry at the temperature below -30°C, $\Delta G^{\ddagger}_{(Tc= 250K)} = 10.6$ kcal mol^{-1}; the Cp' rings cannot be freely rotating, and the η^2-CH_2OMe group must be responsible. The ORTEP in Figure 2 shows that the Ce(η^2-CH_2OMe) fragment is not planar. Perhaps the orientation of the methyl group, C(36), is sufficient to prevent the Cp' group from oscillating resulting in a molecule with C_1 symmetry at low temperature.

Figure 2 shows an ORTEP of $Cp'_2Ce(\eta^2\text{-}CH_2OMe)$; important bond distances and angles are given in the Figure Caption. There is a disorder in the crystal that results from superposition of the two orientations of the individual molecules in a 94:6 distribution, see Experimental Section and Supporting Information for details. The bond distances and angles in the Cp'_2Ce fragment are similar to those previously reported for this fragment.[4a,5,7] The $Ce(\eta^2\text{-}CH_2OMe)$ fragment is not planar since the dihedral angle formed by intersection of the planes defined by CeO(1)C(35) and O(1)C(35)C(36) is 164°. The Ce-C(35) distance of 2.488(4) Å is shorter than that found in $(C_5Me_5)_2Ce[CH(SiMe_3)_2]$, 2.535 Å,[8] and $(C_5Me_5)_2CeCH_2Ph$, 2.596(5)Å.[9] The Ce-O distance of 2.406(2) Å is shorter than the Ce-O distance in $Cp'_2CeO_2S(O)(CF_3)$, where the four independent Ce-O distances in the two individual molecules in the unit cell average to 2.601±0.008 Å[10] but longer than that in $(C_5Me_5)CeO[2,6\text{-}(Me_3C)_2C_6H_3)]_2$ where the Ce-O distance is 2.253 ± 0.002 Å,[11] or in the cis and trans enediolate isomers of $Cp'_2CeOCH{=}CHOCeCp'_2$ where the Ce-O distances are 2.171 ± 0.001 Å and 2.118(3) Å, respectively.[4a]

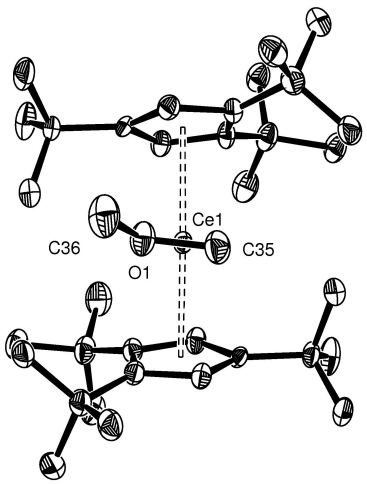

Figure 2. ORTEP of [1,2,4-$(Me_3C)_3C_5H_2]_2CeCH_2OMe$, 50% probability ellipsoids. The non-hydrogen atoms are refined anisotropically and the hydrogen atoms (not shown) are included in calculated positions but not refined: Ce-C_{ave} = 2.84 ± 0.05 Å, range = 2.778(3) to 2.926(3) Å, Ce-C(ring centroid) = 2.57 Å, Cp'(ring centroid)-Ce-Cp'(ring centroid) = 147°, Ce-C(35) = 2.488(4) Å, Ce-O = 2.406(2) Å, C(35)-O = 1.466(4) Å, C(36)-O = 1.414 (4) Å, Ce-O-C(35) = 75.7(2)°, Ce-C(35)-O = 69.5(2)°, C(36)-O-C(35) = 117.2(3)°, C(36)-O-Ce = 160.3(2)°.

Two other structural comparisons are particularly revealing relative to the electronic structure of the methoxymethylene fragment. In organic molecules containing the Me-OC(sp^3) fragment, the average C-O distance is 1.416 Å,[12] which is identical to the C(36)-O(1) distance in the methoxymethyl derivative; the C(35)-O(1) distance of 1.466(4) Å is 0.05 Å longer. Further, the C-O bond in the H_3C-OR group lengthens by 0.12 Å when it is deprotonated at the α-carbon atom as shown by calculations on the hypothetical gas phase molecule $LiCH_2OH$ relative to CH_3OH.[13] The lengthening of the C-O bond is interpreted as arising from increased carbene character in the methylene carbon of the CH_2OH anion. In another comparison, the crystal structure of the methoxymethyl complex, $Cp_2Zr(Cl)(\eta^2$-$CH_2OMe)$, shows that the CH_2-O distance of 1.414(6)Å is shorter than that of the CH_3-O distance of 1.449(6) Å.[14] The crystal structure of the benzyloxymethyl complex, $Cp_2Zr(Cl)(\eta^2$-$CH_2OCH_2Ph)$, shows that the CH_2-O distance is 1.455(8) Å and close to that of the O-C(benzyl) distance which is 1.456(7) Å.[15] These distances are therefore rather different from those in $Cp'_2Ce(\eta^2$-$CH_2OMe)$, Figure 1. In addition, the oxygen atom in $Cp_2Zr(Cl)(\eta^2$-$CH_2OMe)$ is out of the plane defined by the ZrC_2 atoms by 0.51 Å, resulting in the authors description of the $Zr(\eta^2$-$CH_2OMe)$ fragment as an "intramolecularly stabilized onium ylide". This description is strengthened by noting

that the oxygen atom in $[Me_3O][AsF_6]$ is decidedly pyramidal since the angles around oxygen sum to 340°.[16]

Reaction of Cp'$_2$CeH and metallacycle, 1, with CH_3NMe_2.

Unlike the reactions illustrated in eqs 1 and 3, addition of trimethylamine to a C_6D_6 solution of Cp'$_2$CeH does not perturb the chemical shift of the Me_3C-resonances at 20°C in the ^{1}H NMR spectrum. However, mixing trimethylamine with metallacycle, **1**, in C_6D_{12} results in appearance of a new set of Me_3C-resonances in 1:1:1 ratio, though the resonances due to the amine cannot be identified with confidence and a structure analogous to Q_X, X = NMe_2, seems to be a reasonable postulate. After one hour, the ratio of the metallacycle, **1**, to Q_{NMe2} is 1:3 and this ratio changes to 1:6 after a day at 20°C. Heating to 60°C from 2 to 15 days then cooling to room temperature establishes the thermodynamic ratio as 1:1.3. Further support for an equilibrium is obtained by heating metallacycle, **1-d$_{53}$**, with CH_3NMe_2 in C_6D_{12}. After one day at 60°C, resonances in the ^{1}H NMR spectrum due to metallacycle, **1**, increase in intensity at the expense of those in the ^{2}H NMR spectrum. In addition, a triplet is observed in the ^{2}H NMR spectrum due to CH_2DNMe_2, δ = 2.12, J_{CD} = 2Hz. Heating the sample for 33 days at 60°C results in an increase in the paramagnetic resonances due to the $C(CD_3)_2(CD_2H)$ group of the Cp'-rings and their corresponding decrease in the ^{2}H NMR spectrum. The ^{2}H NMR resonance due to trimethylamine-d_x increases in intensity and complexity and the ^{13}C {^{1}H} NMR spectrum contains a resonance as a 1:1:1 pattern at δ = 46.59 and J_{CD} = 20 Hz, in addition to a singlet at δ 46.90 due to CH_2DNMe_2 and CH_3NMe_2, respectively, after 33 days at 60°C. The H for D exchange experiment supports an equilibrium similar to that shown in eq 4, for Q_{NMe2}. Thus, H

for D exchange in CH_3NMe_2 occurs implicating the formation of $Cp'_2CeCH_2NMe_2$, but no resonance due to methane nor Cp'_2CeNMe_2 are observed.

Reactions of Cp'_2CeCH_2OMe with BPh_3

It is clear that H_2 is not able to trap efficiently the CH_2 fragment in Cp'_2CeCH_2OMe. Cyclohexene is not able to trap the CH_2 fragment, since norcarane is not formed when the two reagents are mixed, in contrast to the reaction of the metallacycle, 1, with CH_3F.[1] Thus, another trap that is compatible with the metallocene is needed.[1] Triphenylboron, and indeed BX_3 compounds in general, react with diazomethane, CH_2N_2, with formation of polymethylene, a reaction described by Meerwein eighty years ago;[17] a review of this reaction is available.[18] The specific reaction between BPh_3 and CH_2N_2 yields polymeric material and $(Ph_{3-x})B(CH_2Ph)_x$, since on reaction with hydrogen peroxide, PhOH and $PhCH_2OH$ are formed.[19] Two related reactions should be mentioned; reaction of Ph_3PCH_2 and BPh_3 yields a 1:1 adduct that gives $(PhCH_2)_3B$, Ph_3BPPh_3 and PPh_3 on heating to 205°C[20] and the nitrogenylide Me_3NCH_2•LiBr, and BPh_3 gives $PhCH_2OH$ and PhOH on alkaline hydrogen peroxide hydrolysis.[21] More recently, the adduct between BPh_3 and $Me_2S(O)(CH_2)$ is isolated and after heating and oxidation, $PhCH_2OH$ and PhOH are obtained.[22] Thus, BPh_3 appears to be an efficient trap for the CH_2 fragment, presumably by forming a Lewis acid-base adduct that subsequently rearranges to a benzylboron compound. Although the perfluoro derivative, $(C_6F_5)_3B$, is a stronger Lewis acid it is not compatible with Cp'_2CeH.[23] The utility of BPh_3 as a trap for CH_2 in Cp'_2CeCH_2OMe is outlined next.

Mixing Cp'_2CeCH_2OMe with BPh_3 in an NMR tube in C_6D_6 at 20°C results in disappearance of the resonances due to the methoxymethyl derivative and appearance

of resonances due to Cp'_2CeOMe within 10 minutes. Although resonances that may be attributed to an arylboron derivative are apparent in the spectrum, their identification is not clear cut; the ^{11}B NMR spectrum offers no help since the quantity of $(Ph_{3-x})B(CH_2Ph)_x$ is small and the paramagnetism of the cerium compound is likely to shift the broadened resonance. However, hydrolysis of the solution with alkaline hydrogen peroxide and examination of the hydrolysate by GCMS conclusively shows that $PhCH_2OH$ and PhOH, in addition to Cp'H, are formed. Thus BPh_3 is able to abstract the CH_2 group resulting in the net reaction shown in eq 5.

$$Cp'_2CeCH_2OMe + BPh_3 \rightarrow Cp'_2CeOMe + Ph_2BCH_2Ph \quad (5)$$

In the reaction illustrated in eq 5, BPh_3 is a better trap for CH_2 than H_2 since the methoxymethyl derivative is formed in presence of H_2, eq 3. This observation begets the question of which reagent is a better trap for a CH_2 group when the postulated compound Cp'_2CeCH_2X, Q_X, is neither detected nor isolated, i.e., the reaction shown in eq 1. This is an important question since the only experimental evidence for formation of Cp'_2CeCH_2F is derived from experiments in which H_2 is absent, i.e., eq 2. The success of this type of experiment requires that BPh_3 does not react irreversibly with Cp'_2CeH.

An NMR tube experiment shows that mixing BPh_3 and Cp'_2CeH in C_6D_6 results in a rapid color change from purple to yellow and disappearance of the resonances due to Cp'_2CeH. On a synthetic scale, addition of Cp'_2CeH and BPh_3 in toluene at room temperature results in the appearance of a yellow solution and yellow crystals form on standing overnight. The crystals are due to formation of a 1:1 adduct, whose crystal structure is shown in the ORTEP in Figure 3. Some bond distances and angles are given in the Figure Caption.

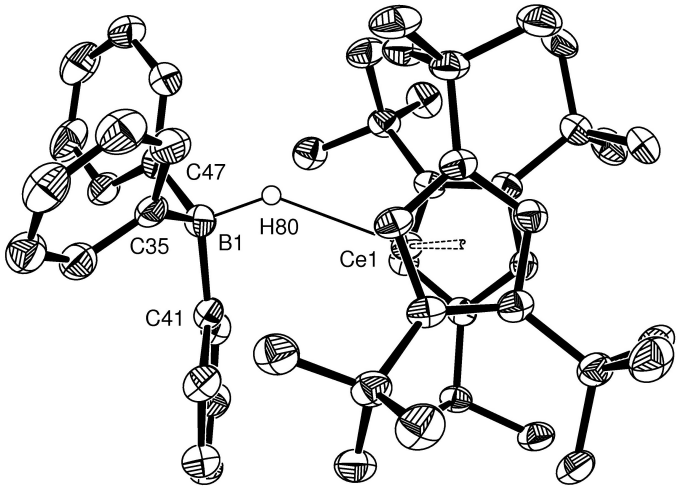

Figure 3. ORTEP of $[1,2,4\text{-}(Me_3C)_3C_5H_2]_2Ce(H)(BPh_3)$, 50% probability ellipsoids except for H(80). All non- hydrogen atoms are refined anisotropically and all hydrogen atoms, except H(80), are placed in calculated positions and not refined. H(80) is located in the difference Fourier map and refined isotropically. Some bond distances and angles are: $Ce\text{-}C(Cp')_{ave} = 2.82 \pm 0.09$ Å, $Ce\text{-}Cp'(centroid)_{ave} = 2.54$ Å, Cp'(centroid)-Ce-Cp'(centroid) = 136°, Ce-H(80) = 2.37(3) Å, Ce-B = 3.423(3) Å, B-H(80) = 1.26(3) Å, Ce-H(80)-B = 139(1)°.

A comparison between the geometrical parameters in Cp'_2CeH, the adduct with BPh_3, and BPh_3, is shown in Table 1. The cyclopentadienyl ring carbon atoms are nearly eclipsed in the starting hydride and the Cp'(centroid)-Ce-Cp'(centroid) angle is 155°.[5] The refined position of the hydride atom lies off the C_2-axis of the metallocene. When BPh_3 interacts with the hydride, the Cp'(centroid)-Ce-Cp'(centroid) angle closes to 136°, the cyclopentadienyl-ring carbons on the Cp'-rings are now staggered, but the Cp'(centroid)-Ce distances are essentially equal in the two structures. The $HBPh_3$ group does not lie on the C_2-axis of the complex, but it

is oblique to the Cp'_2Ce fragment with a Ce-H(80)-B angle of 139(1)°. This orientation forces the BPh_3 group close to the Cp'_2Ce fragment with a Ce···B distance of 3.423(3) Å. The Ce-H distance in the complex increases to 2.35 Å from 1.90 Å in the BPh_3-free complex and the H-B distance is 1.26 Å. The refined H-B distance seems reasonable since an equivalent distance of 1.34 Å is found in $(C_5H_5)_2V(H)(B(C_6F_5)_3)$, where the V-H-B angle is 153°.[24] The H-B distance tends to be longer by about 0.2 Å when the HBR_3 group is inner sphere rather than outer sphere since, for example, the H-B distance in $[(C_5H_5)_2V(CO)_2][HB(C_6F_5)_3]$ is 1.14(2) Å[25] and 1.06(6) Å in $[(C_5Me_5)_2ZrH][HB(C_6F_5)_3]$.[26] The B-C distance lengthens by 0.05 Å on complex formation and the C-B-C angles contract from 120° in planar BPh_3, in which the phenyl groups are orientated as the blades of a propellar, to 111.8 ± 3.2° (ave.) in the complex. However, the C-B-C angles are unequal in the adduct: they range from 107.0(2)° for C(35)-B-C(47) to 114.3(3)° and 114.0(3)° for the other two angles at boron. The geometrical parameters in $Cp'_2Ce(H)(BPh_3)$ are consistent with the view that the Ce-H-BPh_3 interaction is a 3 center-2 electron bond and the obtuse Ce-H-B angle implies a closed 3-center interaction in the solid state, i.e., there is electron density shared between the Ce and B atoms.[27]

Table 1. Comparison of Bond Lengths and Angles in Cp'_2CeH, $Cp'_2Ce(H)(BPh_3)$ and BPh_3.

	Cp'_2CeH	$Cp'_2Ce(H)(BPh_3)$	BPh_3[c]
$Ce\text{-}C(Cp')_{ave}$,[a] Å	2.81 ± 0.02	2.82 ± 0.09	
Ce-C(Cp') range, Å	2.757(7) to 2.840(6)	2.713(3) to 2.933(3)	
$Ce\text{-}Cp'(centroid)_{ave}$. Å	2.53	2.54	

Orientation[b]	Eclipsed	staggered	
Cp'(centroid)-Ce-Cp'(centroid), °	155	136	
B-C, Å		1.631 ± 0.008	1.580 ± 0.005
C-B-C, °		111.8 ± 3.2	120

[a)] For averaged values, the deviation is the average deviation from the mean.

[b)] The relative orientation of the carbon atoms in the Cp'-rings.

[c)] Zettler, F.; Hausen, H. D.; Hess , H. *J. Organomet. Chem.* **1974**, *72*, 157.

In C_6D_6 solution the interaction persists, since at 20°C, the resonances due to $Cp'_2Ce(H)(BPh_3)$ and those due to added BPh_3 are observed as separate resonances. The variable temperature ^1H NMR spectra of $Cp'_2Ce(H)(BPh_3)$ are shown as a δ vs 1/T plot in Figure 4. At temperatures below 332K (1/T ≅ 0.003) separate resonances are observed for free and coordinated BPh_3, the para-H resonances are easily distinguished in the adduct and free BPh_3. Below that temperature the Me_3C-groups on the Cp'-rings appear in a 1:1:1 ratio consistent with a complex with C_s symmetry. At higher temperatures, two of the Me_3C-resonances coalesce, due to the equilibrium illustrated by eq 6, that averages the BPh_3 environments. Thus, at temperatures above T = 330K, some BPh_3 is present in solution and may function as a trapping reagent.

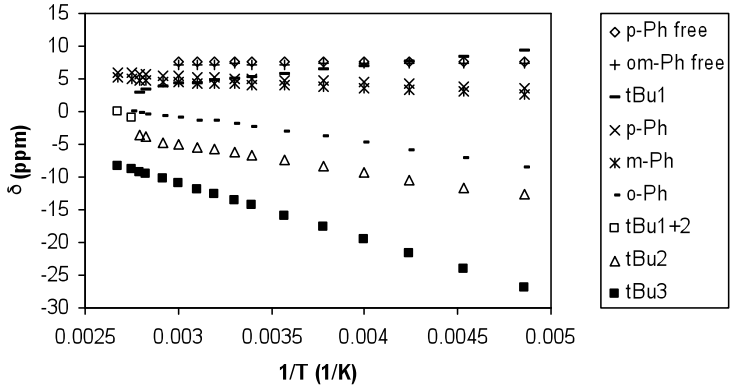

Figure 4. δ vs. 1/T plot for $Cp'_2Ce(H)(BPh_3)$.

$$Cp'_2Ce(H)(BPh_3) \rightleftharpoons Cp'_2CeH + BPh_3 \qquad (6)$$

Accordingly, mixing $Cp'_2Ce(H)(BPh_3)$ with CH_3F results in formation of Cp'_2CeF and free BPh_3. The conversion is only about 20% after 10 minutes and therefore the rate of reaction decreases in the adduct. In a separate experiment, the resonances due to Cp'_2CeF are not perturbed in presence of BPh_3 at 20°C. Similarly, addition of CH_3Br to $Cp'_2(H)(BPh_3)$ in C_6D_6 results in formation of Cp'_2CeBr. Hydrolysis of the solution with alkaline hydrogen peroxide and examination by GCMS shows that only phenol is formed. Hence, at the concentrations used, BPh_3 does not compete with dihydrogen for the CH_2-fragment.

As shown in an earlier article,[5] metallacycle, **1-d$_{53}$**, is readily prepared by exposing **1-d$_0$** to C_6D_6 solvent. The reverse reaction, *viz.*, metallacycle, **1-d$_{53}$** in presence of C_6H_6 gives **1-d$_0$** and $C_6H_{6-x}D_x$ implies that aryl CH-bonds in BPh_3 will undergo exchange of H for D with **1-d$_{53}$**. This expectation is fulfilled, since mixing **1-d$_{53}$** with BPh_3 in an NMR tube in C_6D_{12} at 20°C results in a decrease in intensity of the resonances due to the $(CD_3)_3C$-groups in the ^2H NMR spectrum and an increase in intensity of the resonances of the para-H and meta-H sites; those on the ortho-H sites are not affected. After 2 days at 60°C, the ratio o-H:m-H:p-H is 2.0:0.4:0.09 and after 11 days at 60°C the ratio is 2.0:0.12:0.025.

Other reactions of $Cp'_2Ce(\eta^2\text{-}CH_2OMe)$, Q_{OMe}.

Several additional reactions of the methoxymethyl derivative are summarized in the Scheme and outlined in this section. Exposure of $Cp'_2Ce(\eta^2\text{-}CH_2OMe)$ to D_2

results in deuterium being detected in two positions; the Me_3C-groups of the Cp'-ring and the Ce-D sites, i.e., (Cp')(Cp'-d_1)CeD, as shown by the intensity changes in the ^1H and ^2D NMR spectra. In addition, some deuterium accumulates in Me_2O. These results are consistent with the equilibrium illustrated in eq 4 and in the Scheme.

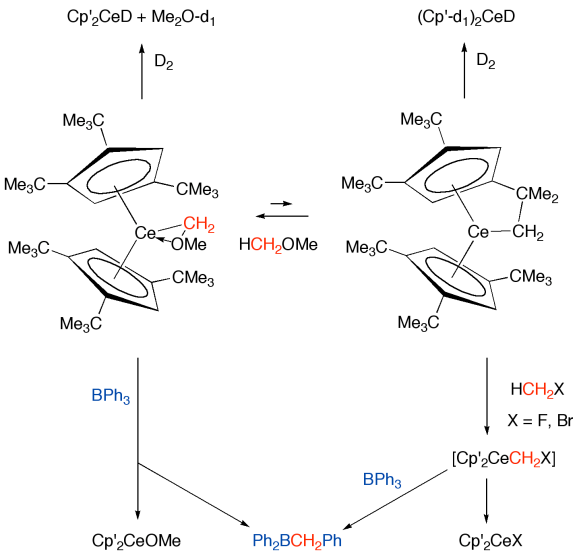

Scheme

The methoxymethyl derivative reacts with MeX, X = F or Br, as shown in the Scheme. In the case of MeBr, resonances due to Q_{OMe}, Cp'$_2$CeBr, Cp'$_2$CeOMe and Q_{Br} are observed after 1 day at 20°C in a ratio of 8:8:1:2 along with Me_2O. After 4 days, only resonances due to Cp'$_2$CeBr and Me_2O are observed. In a separate experiment, Cp'$_2$OMe is not converted to Cp'$_2$CeBr by MeBr, which shows that the disappearance of the small amount of Cp'$_2$CeOMe is not due to reaction with MeBr. Methylfluoride also reacts with Cp'$_2$Ce(η^2-CH_2OMe) but the rate is slower that that of MeBr. After 2 days at 20°C, only resonances due to Cp'$_2$CeCH_2OMe and Cp'$_2$CeF are observed, but

heating for 1 day at 60°C, resonances due to Cp'_2CeOMe appear. In a separate experiment, $Cp_2'CeOMe$ and MeF do not react. After 9 days at 60°C, the relative ratio of Cp'_2CeF and Cp'_2CeOMe is 1.5:1 and the resonances due to $Cp'_2Ce(\eta^2\text{-}CH_2OMe)$ are gone. This result is also consistent with the equilibrium reaction shown in the Scheme.

Computational studies

The metallocene used in the experimental studies, Cp'_2CeH was modeled by $(C_5H_5)_2CeH$, symbolized as [Ce]H, as in earlier articles.[1,4a, 5] The results obtained with CH_3F are incorporated into this article for completeness. The free energy profiles for the reaction of CH_3X with [Ce]H to form [Ce]X and CH_4 are shown in Figure 5; the activation barrier is defined as the difference in free energy between the reactant and the transition state and symbolized as $\Delta G^{\ddagger}$.

The metathesis pathway with a transition state shown as **I** in the Introduction, has an activation barrier of 31.1 kcal mol^{-1} for CH_3F.[1] The calculated activation barriers are 30.4 kcal mol^{-1} for CH_3I and 43.5 kcal mol^{-1} for CH_3OMe. These two systems are representative of the series of CH_3X species discussed in this article and the metathesis pathway is unlikely to be followed. The pathway that proceeds *via* a transition state of type **II** and on to intermediate **III** was proposed in the case of CH_3F and this pathway is explored as an alternative pathway below. The activation energy for the CH activation steps in the five reactions is similar but the activation energy for trapping of CH_2 and formation of Cp_2CeX is strongly dependent on the identity of X, Figure 5.

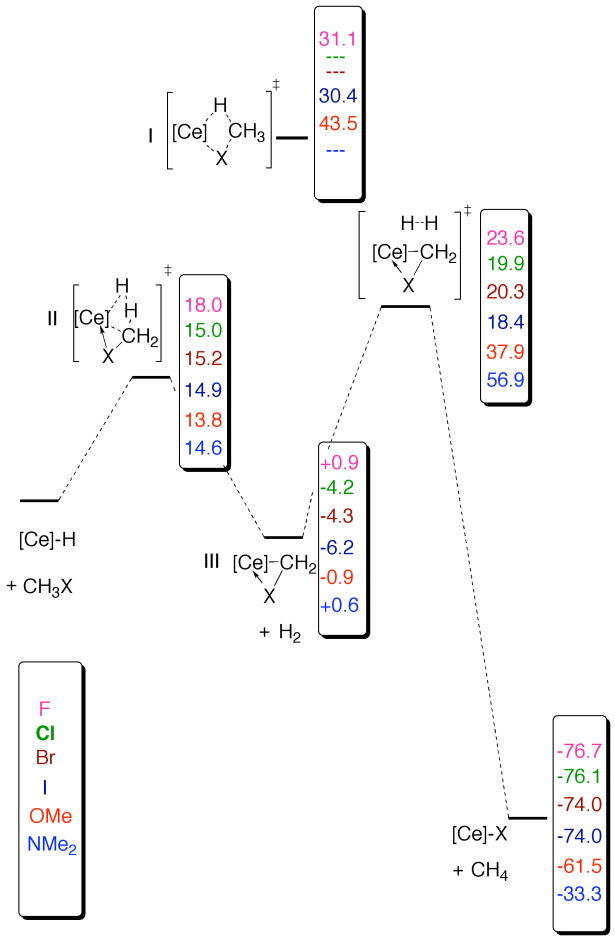

Figure 5. Free energy profiles, in kcal mol^{-1}, for the reaction of Cp_2CeH, [Ce]H, and CH_3X to form [Ce]X and CH_4 (X = F, Cl, Br, I, OMe, NMe_2). The adduct between CH_3X and [Ce]H is not shown.

The reaction begins by coordination of CH_3X to [Ce]H by a lone pair on X. Coordination just compensates the loss of translational entropy in the system and the free energy of the adducts is similar to that of the separated reactants; for this reason the adducts are not shown on Figure 5. From the adduct, the hydrogen atom transfers as a proton from the methyl group to the hydride as described for the CH_3F reaction. At the transition state, the carbon atom, the hydrogen atom that is leaving the methyl group, and the hydrogen atom attached to Cp_2Ce are essentially co-linear as shown in Figure 6a for X = OMe where the H···H···C angle is 170°. The transfer of the proton

results in the formation of H_2 and [Ce](η^2-CH_2X) in which the carbon and X atom of the CH_2X group are bonded to the cerium atom. The transition state for the insertion of CH_2 into H_2 for X = OMe is shown in Figure 6b.

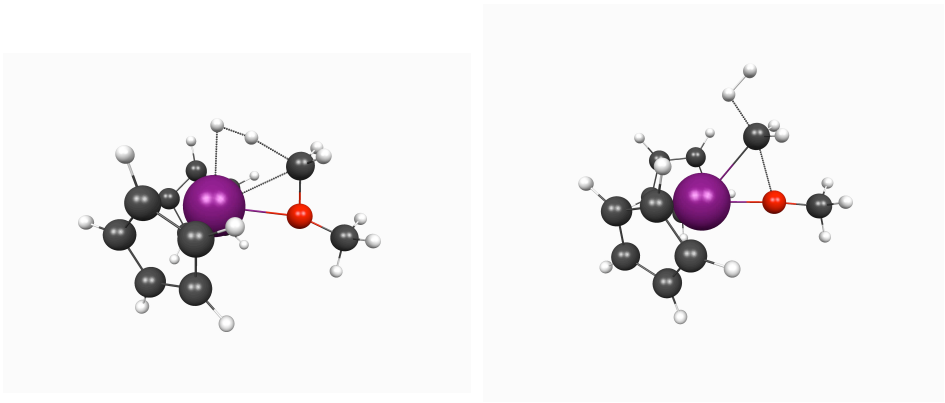

(a) (b)

Figure 6. Transition states for the formation of CH_4 and [Ce]OMe from CH_3OMe and [Ce]H. (a) elimination of H_2 with a H···H···C angle of 170°, (b) addition of H_2 to the η^2-CH_2OMe group with formation of [Ce]OMe.

The activation barrier ($\Delta G^{\ddagger}$) for the proton transfer reactions is similar for all X: the lowest value of 13.8 kcal mol^{-1} is obtained for X = OMe, the highest value of 18 kcal mol^{-1} is obtained for F and values for X = Cl, Br, I and NMe_2 are in between at about 15 kcal mol^{-1}. The values do not follow the experimental gas phase proton dissociation enthalpies for CH_3X, since the values as a function of X, in kcal mol^{-1} are NMe_2 (> 406), OMe (407), Cl (396), Br (393), I (391).[28] Thus, the activation barrier is not just determined by the acidity of the α-CH bond, even though the relative acidity is the primary reason for the higher activation energy when H_2 and CH_4 are compared, and the identity of X plays a role in determining the barrier.[1] The free energy of formation of [Ce](η^2-CH_2X) is only mildly influenced by X with the heavier halides

and the methoxy group being slightly more stable than the reactant and the fluoride and NMe_2 slightly less; therefore the reactants, [Ce]H and CH_3X, and [Ce](η^2-CH_2X) are essentially isoenergetic.

The activation barriers for insertion of CH_2 into H_2 vary over a large range of values. For the halides, Cl, Br and I, the activation barriers are about 24 kcal mol^{-1}. A significantly higher activation barrier of 39 kcal mol^{-1} is calculated for X = OMe and the barrier is even higher, 56 kcal mol^{-1}, for X = NMe_2. The formation of [Ce]X and CH_4 is strongly exoergic for all of the X substituents but the nature of X influences the value of ΔG of the reaction which decreases in the order F, Cl, Br, I > OMe >> NMe_2. Figure 5 shows a clear relationship between the activation energies for insertion of CH_2 into H_2 and the change in free energy of reaction since the highest activation barriers are associated with the lowest thermodynamic driving force. The proton transfer step is a low activation barrier process for all CH_3X reactants but the insertion of CH_2 into dihydrogen proceeds with a higher barrier and is therefore rate determining.

The carbon atom that is part of the three-membered ring, [Ce](η^2-CH_2X), is a carbenoid,[29] since it shows reactions associated with a carbene, for example, insertion into H_2, as well as that of an alkyl group, for example, as a proton acceptor, see Scheme. However, the identity of X plays an role in the height of the activation barrier since the CH_2 group is a carbenoid and not a free carbene, which inserts into H_2 without an energy barrier.[30] The values of the activation energy become progressively higher as X changes from F to OMe and to NMe_2. In the latter example, a calculated activation barrier of 56 kcal mol^{-1} is prohibitively high consistent with the experimental observation that [Ce]NMe_2 does not form from CH_3NMe_2, even though

the net reaction is exoergic by -33 kcal mol^{-1}. In the case of [Ce](η^2-CH_2OMe) going to [Ce](OMe) and CH_4, the calculated activation barrier of 39 kcal mol^{-1} seems too high for an experimental reaction that occurs, albeit slowly at 20°C, but consistent with the experimental fact that Cp'$_2$CeCH_2OMe is an isolable compound. Similarly, an activation barrier of 24 kcal mol^{-1} when X is F, also seems excessive for a net reaction that is rapid at 20°C.

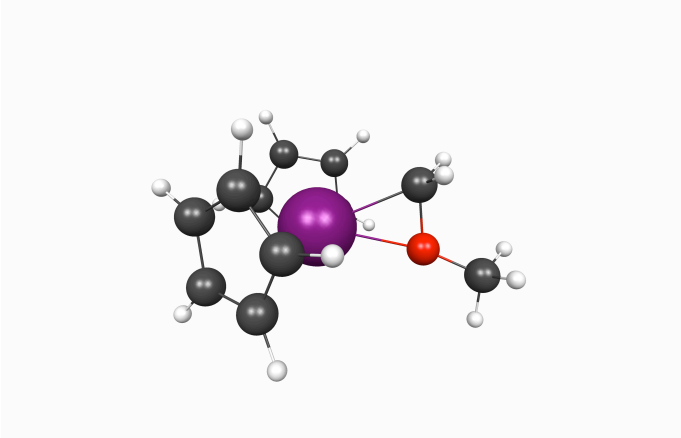

Figure 7. Optimized structure of [Ce](η^2-CH_2OMe).

The calculated structures of Ce(η^2-CH_2X) when X is a halide are very similar to those for X = F.[1] Descending the halide series results in longer C-X bonds and an increase in the Ce-C-X angle that varies from 71° for F to 86° for I. For X = OMe, the Ce-C-O angle is close to that for X = F while for X = NMe_2, the Ce-C-N angle is 76°, midway between that for F (71°) and for X = Cl (80°). An important aspect of the calculated structure, which is not obtained from the crystal structure of Cp'$_2$$CH_2OMe$, is the position of the two hydrogen atoms on the methylene group, Figure 7. This geometrical parameter is related to the hybridization at the carbon atom and therefore to the carbenoid character in the CH_2X group. For all X, the two hydrogen atoms are oriented in such a way that the Ce-C axis is essentially in the plane defined by carbon and the two hydrogen atoms. The H-C-H angle is close to 120° for all X. These results show that the hybridization of carbon is sp^2 and that the C-X bond is

essentially constructed from a p-orbital on the carbon atom. Similar geometrical features have been found in the calculated structures of $LiCH_2X$ (X = F, Cl, Br, I, OH, OMe, NH_2).[31] Thus changing X does not change the orientation of the CH_2 relative to the Ce-C bond nor the H-C-H angle, but changing X changes the Ce-C-X angle, which is the smallest for F (71°) and largest for I (86°). This difference is a consequence of the increasing C-X bond length down the halide column.

The distortion of [Ce](η^2-CH_2X) on going to the transition state as H_2 traps the CH_2 fragment is influenced by X as shown in Table 2. The distortions are very similar in the case of Cl, Br, and I; the Ce-C distance increases by around 0.1 Å, the C-X distance increases by about 0.5 Å, while the Ce-X distance decreases by around 0.1 Å. Different and larger distortions are found for X = F, OMe and NMe_2. In the case of F, the Ce-C distance increases by almost 0.4 Å, four times that found for the heavier halide, while the increase in the C-F distance of 0.47 Å is marginally smaller than that for the other halides. The Ce-F bond does not shorten much on going from [Ce](η^2-CH_2F) to the transition state. In the case of OMe and NMe_2, the Ce-C distance increases as found for the heavy halides, but the C-X bond increases more (0.66 Å and 0.8 Å for OMe and NMe_2 respectively). Another difference between the halides and the OMe or NMe_2 cases is the H···H distance at the transition state; the H···H distance is 0.80 Å for all of the halides but it increases from 0.83 to 0.88 Å when X is OMe or NMe_2, respectively.

Table 2. All bond distances are in Å. The first row of each cell gives the distances in the ground state (gs) of the three-membered ring and the second row gives the distances in the transition states (ts) for insertion of CH_2 into H_2. a) The changes in the

bond lengths are given as Δ(Ce-C), Δ(C-X) and Δ(Ce-X) where a positive number is an elongation of the bond from the reactant to the transition state. b) The C···H distance given is the shorter of the two C···H distances at the transition state. c) The H···H distance is given at the transition state.

		Ce-C	C-X	Ce-X	Δ(Ce-C)[a]	Δ(C-X)[a]	Δ(Ce-X)[a]	C···H[b]	H···H[c]
F	gs	2.476	1.510	2.505	+0.374	+0.466	-0.06	-	-
	ts	2.850	1.976	2.445				1.516	0.798
Cl	gs	2.547	1.897	2.904	+0.099	+0.524	-0.122	-	-
	ts	2.646	2.421	2.782				1.485	0.804
Br	gs	2.554	2.045	3.07	+0.101	+0.530	-0.119	-	-
	ts	2.655	2.575	2.951				1.465	0.810
I	gs	2.559	2.277	3.300	+0.105	+0.516	-0.111	-	-
	ts	2.664	2.793	3.189				1.452	0.814
OMe	gs	2.510	1.461	2.445	+0.107	+0.656	-0.187	-	-
	ts	2.617	2.117	2.258				1.407	0.829
NMe_2	gs	2.508	1.490	2.587	+0.118	+0.814	-0.175	-	-
	ts	2.626	2.304	2.412				1.314	0.877

Reaction of [Ce](η^2-CH_2OMe) with BPh_3

The free energy profile for the reaction of [Ce](η^2-CH_2OMe) with BPh_3 is shown in Figure 8; the structure of the intermediate and the transition state are shown in the Supporting Information. The reaction begins by coordination of BPh_3 to the methylene group of [Ce](η^2-CH_2OMe) yielding a complex where the methylene group is bonded to boron not cerium. Thus, BPh_3 successfully competes with [Ce] for

the density at the carbenoid carbon. However, this complex has a free energy of 15.7 kcal mol^{-1} higher than the separated species [Ce](η^2-CH_2OMe) and BPh_3 and the difference is mostly due to loss in translational entropy since the energy, E, of the adduct between [Ce](η^2-CH_2OMe) and BPh_3 is equal to that of the separated species. From this adduct, [Ce]OMe and Ph_2BCH_2Ph are formed in a concerted step with an activation barrier of 29 kcal mol^{-1} relative to separated reactants [Ce]H, CH_3OMe and BPh_3. This activation barrier is lower than that of 39 kcal mol^{-1} for the insertion of the methylene group into H_2 showing that BPh_3 is a more efficient trap of the methylene group than is H_2, a result that is supported by experiment. At the transition state, the C-O bond length of 2.07 Å shows that the bond is essentially cleaved. The ylide $Ph_3B^{(+)}CH_2^{(-)}$ is not an intermediate; the geometry of the transition state shows that one phenyl group is bending over the B-CH_2 bond with a C-B-C(phenyl) angle of 79° for one of the phenyl group and 115° for the two other angles. Insertion of the CH_2 group into the B-C bond is therefore concerted with the C-O bond cleavage. The net reaction for [Ce](η^2-CH_2OMe) and BPh_3 forming [Ce]OMe and Ph_2BCH_2Ph is exoergic by 41 kcal mol^{-1}.

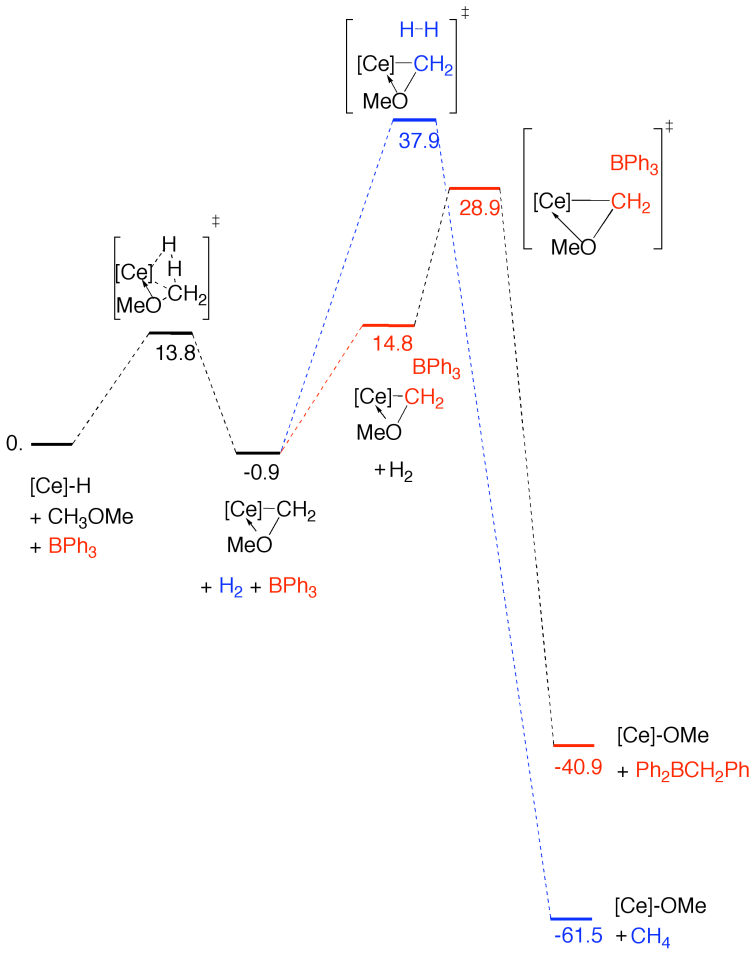

Figure 8. The free energy profile, in kcal mol^{-1}, for the reaction of [Ce]H, CH_3OMe, and BPh_3. The free energy profile for the reaction of [Ce]H and CH_3OMe, Figure 5, is added for comparison.

Discussion

The reactions between Cp'_2CeH and CH_3X compounds fall into three distinct classes, depending on the identity of X. When X is a halide, F, Cl, Br or I, class a, the net reaction is a simple H for X exchange that proceeds rapidly without any intermediates detected by ^1H NMR spectroscopy. Class b is when X is OMe, as the reaction with Cp'_2CeH gives the H for CH_2OMe exchange product, $Cp'_2Ce(\eta^2$-

CH_2OMe), as an isolable compound and H_2. The ^1H NMR chemical shifts of the Me_3C-groups at 20°C have similar values as those observed in the reaction between the metallacycle, **1**, with CH_3X, X = Cl, Br, and I, consistent with the postulate that all of these reactions proceed through a common intermediate Q_X, eq 2 and 3. Since the reaction with metallacycle, **1**, does not generate H_2, the intermediates Q_X are detected, which implies that the barrier for conversion of Q_X to Cp'_2CeX and CH_4 in presence of H_2, is lower when X is Cl, Br, I than when X is OMe. Class c is the reaction with CH_3NMe_2. No net reaction is observed but deuterium labeling experiments show that H for D exchange occurs in trimethylamine, implying that intermediate Q_{NMe2} forms and that Cp'_2CeH and Q_{NMe2} are in equilibrium. This implies that the H for D exchange proceeds with a low barrier but that the conversion of Q_{NMe2} to Cp'_2CeNMe_2 has an impossibly high barrier. The reactions between Cp'_2CeH and CH_3X proceed by a low barrier intermolecular α–CH activation followed by ejection of the CH_2 fragment and capture by H_2, a higher barrier process whose value is strongly correlated with the identity of X. The latter barriers define the classes a, b or c.

The net reaction of Cp'_2CeH and CH_3X, eq 1, is thermodynamically favorable since the experimentally determined or estimated changes in the enthalpy are exothermic for the reaction shown in eq 7.[32]

$(C_5Me_5)_2SmH + MeX \rightarrow (C_5Me_5)_2SmX + MeH$ (7)

ΔH (kcal mol^{-1}): X = Cl, -66; Br, -65; I, -64; OMe, -48; NMe_2, -22.

Although the experimental values are only available for the samarium metallocenes, the trends in ΔH should be similar when the metal is a lanthanide in general, and when the metal is cerium in the present article. As shown in the experimental and calculational results described in this article, even though the net reaction is

thermodynamically favorable for all X, the reactions are under kinetic control. The calculated potential energy surfaces for the gas phase reaction between Cp_2CeH and MeX parallel and therefore illuminate the experimental reactions between Cp'_2CeH and MeX. The calculated free energy profiles show that the net reaction is exoergic, in agreement with experiments, and that a σ-bond metathesis transition state has a higher activation barrier.

A mechanism that is calculated to proceed by a lower energy pathway for X = a halide, is a two-step process in which the first step is a α-CH activation that forms Q_X and H_2, followed by trapping of CH_2 by H_2, that proceeds with a higher activation barrier, its height defining the classification as either a, b, or c. Since the rate controlling elementary step is the conversion of Q_X into the products, the structure and bonding in Q_X is of paramount importance. Accordingly, the structure is calculated for all of the X's studied and calibrated with the experimental geometry observed in $Cp'_2Ce(\eta^2\text{-}CH_2OMe)$. In general Q_X, $Cp'_2Ce(\eta^2\text{-}CH_2OMe)$, is a three-membered ring in which the carbon atom is sp^2-hybridized and therefore the CH_2 fragment is a carbenoid. The bonding between the carbene and M···X, when M is electropositive and X is electronegative, is maximized when the σ-lone pair of the carbene interacts with M and the empty 2p orbital of the carbene interacts with X; this is the basis of Bent's rule.[33] At the transition state, the C-X bond lengthens as the Ce-X bond forms. The orientation of the CH_2 group is such that the carbon p-orbital points toward dihydrogen. The activation barrier for trapping of CH_2 by H_2 parallels the free energy of reaction. When X is a halide, the change in the C-X bond distance going from $[Ce][\eta^2\text{-}CH_2X)$ to the transition state is similar for all halides but larger when X is OMe and NMe_2. In addition, the H···H distance in the transition state is longer when X is OMe and NMe_2. Thus, the transition state for trapping of CH_2 by H_2 is higher in

energy when X is OMe and NMe_2, which in turn implies that the CH_2 fragment in [Ce][η^2-CH_2X) is closer to a free carbene when X is a halide.

Conclusion

At first glance, the reactions illustrated in eq 1 are simple H for X metathesis reactions. The reactions, however, are deceptively simple since the mechanism deduced by DFT calculations and trapping experiments is not a one-step, synchronous σ-bond metathesis, but a two-step process in which a relatively rapid α-CH activation results in formation of H_2 and $Cp_2Ce(\eta^2\text{-}CH_2X)$, in which the CH_2 fragment is a carbenoid. The reactivity patterns are therefore correlated with how closely the carbenoid fragment resembles a free carbene fragment, on one hand, and a methyl group on the other: the closer the resemblance to CH_2, the lower the barrier. The calculational and experimental studies outlined in this and an earlier article[1] show that the mechanisms of the H for X exchange reaction between Cp'_2CeH and CH_3X is a two-step pathway, and this is a general reactivity pattern. The reactants, CH_3X, studied in these articles have only α-CH bonds and therefore the question of selectivity does not arise. It will be of interest to examine CH_3CH_2X reactants in which the choice between α- and β-CH activation processes are available; this selectivity issue will be addressed in another article.

Experimental Section

General

All manipulations were performed under an inert atmosphere using standard Schlenk and dry box techniques. All solvents were dried and distilled from sodium or

sodium benzophenoneketyl. Anhydrous methylchloride, methylbromide, dimethylether, and trimethylamine were used without further purification. Methyliodide was obtained commercially and purified by distillation onto activated 4 Å molecular sieves. Triphenylboron was obtained commercially and purified by sublimation under dynamic vacuum. NMR spectra were recorded on Bruker AV-300 or AV-400 spectrometers at 20°C in the solvent specified. J-Young NMR tubes were used for all NMR tube experiments. Electron impact mass spectrometry and elemental analyses were performed by the microanalytical facility at the University of California, Berkeley. The abbreviation Cp' is used for the 1,2,4-tri-*tert*-butylcyclopentadienyl ligand. Unless otherwise specified, samples for GC-MS were prepared by adding a drop of nitrogen-purged H_2O, agitating, and allowing the samples to stand closed for 10 min. The samples were then dried over magnesium sulfate, filtered, and diluted ten-fold with pentane. A 1 μL sample was injected into a HP6890 GC system with a J&W DB-XLB universal non-polar column, attached to an HP5973 Mass Selective Detector. For samples hydrolyzed with basic hydrogen peroxide, a 3N aqueous NaOH solution was sparged for 10 minutes with nitrogen, and a drop was added to the sample under nitrogen flush. The sample was closed, agitated, and allowed to stand for 10 minutes, after which time a drop of 30% aqueous H_2O_2 was added, the sample was closed briefly, agitated, then opened and allowed to stand for five minutes. The organic and aqueous layers were separated, and the aqueous layer was extracted twice with diethylether. The combined organic layers were then analyzed by GC MS as before.

Cp'$_2$CeCH$_2$OMe: Cp'$_2$CeH[5] (0.5g, 0.82 mmol) was dissolved in pentane (10 mL). The headspace was evacuated and replaced with dimethylether (1 atm). The solution color changed from purple to red as it was stirred over the course of one hour. The

volume of the solution was reduced to 5 mL under reduced pressure, and the solution was cooled to –15°C, yielding red crystals. Yield, 0.20 g (0.31 mmol, 37%). MP 210-213°C (sample turned deep purple at 135°C, melted at 210-213°C). ^{1}H NMR (C_6D_6, 300MHz): δ 35.38 (4H, $\nu_{1/2}$ = 260 Hz), 26.10 (3H, $\nu_{1/2}$ = 140 Hz), -1.11 (36H, $\nu_{1/2}$ = 730 Hz), -10.90 (18H, $\nu_{1/2}$ = 15 Hz); the CH_2 resonance in the CH_2OMe ligand was not observed. MS: no $(M)^+$ was observed but $(M\text{-}CH_2OMe)^+$ was found *m/z* (calc, found) 605 (100, 100) 606 (39, 52) 607 (17, 22) 608 (6, 10). Anal. Calcd. for $C_{36}H_{63}CeO$: C, 66.32; H, 9.74. Found C, 66.41; H, 10.03. Full crystallographic details are included as Supporting Information. Triclinic cell space group P1(bar): a = 10.4888(5) Å, b = 10.9920(5) Å, c = 15.9639(7) Å, α = 99.137(1)°, β = 104.458(1) °, γ = 95.703(1) °, V = 1740.9(1) Å^3.

Cp'$_2$CeBr: Cp'$_2$CeOTf[5] (0.25g, 0.31 mmol) was dissolved in pentane (10 mL) and Me_3SiBr (120μL, 0.91 mmol) was added *via* syringe. The solution was stirred for one day, then taken to dryness under reduced pressure. The yellow solid was dissolved in pentane and filtered. The yellow solution was concentrated until precipitation occurred, warmed to dissolve the precipitate, then cooled to –15°C, yielding a yellow powder. Yield, 0.095 g (0.13 mmol, 42%). MP 266-270°C. ^{1}H NMR (C_6D_6, 300MHz): δ -2.46 (36H, $\nu_{1/2}$ = 550 Hz), -14.03 (18H, $\nu_{1/2}$ = 170 Hz). MS $(M)^+$ *m/z* (calc, found) 685 (86, 85) 686 (32, 30) 687 (100, 100) 688 (36, 31) 689 (17, 13). Anal. Calcd. for $C_{34}H_{58}CeBr$: C, 59.46; H, 8.51. Found C, 59.61; H, 8.36.

Cp'$_2$CeI: $CeI_3 \bullet 3$ THF[34] (18.1 g, 25.0 mmol) and Cp'$_2$Mg[35] (12.0g, 24.0 mmol) were stirred at reflux in a mixture of pyridine (10 mL) and toluene (100 mL) for 24 hours. The orange-brown suspension was taken to dryness under reduced pressure. The solid residue was loaded into an extraction thimble (dried at 120°C for three days) and extracted with pentane (200 mL) in a Soxhlet extractor for three days. After

12 hours, an orange precipitate appeared in the solvent flask. The extraction was stopped and the flask containing the precipitat was cooled to –15°C, yielding dirty orange powder. The suspension was filtered, and the flask containing the mother liquor was reattached to the extraction apparatus. The extraction was continued until the solution around the extraction thimble was colorless. Recrystallization of the combined orange powder from toluene (100 mL) yielded small, opaque, bright orange crystals. Yield, 10.2 g (14 mmol, 56%). MP 309-311°C. ^{1}H NMR (C_6D_6, 300MHz): δ 3.20 (18H, $\nu_{1/2}$ = 430 Hz), -8.03 (18H, $\nu_{1/2}$ = 430 Hz), -15.14 (18H, $\nu_{1/2}$ = 220 Hz). MS $(M)^+$ *m/z* (calc, found) 733 (100, 100) 734 (37, 37) 735 (19, 19) 736 (6,5). Anal. Calcd. for $C_{34}H_{58}CeI$: C, 55.65; H, 7.96. Found C, 55.76; H, 8.17.

Cp'$_2$CeHBPh$_3$: Cp'$_2$CeH[5] (0.5 g, 0.72 mmol) and BPh_3 (0.2 g, 0.82 mmol) were dissolved in toluene (10 mL). The clear yellow solution was allowed to stand at 19°C overnight, resulting in yellow crystals. The ^{1}H NMR spectrum of the crystals in C_6D_6 indicated the presence of toluene of crystallization. Yield, 0.50 g (0.53 mmol, 74%). MP 202-205°C. ^{1}H NMR (C_7D_8, 300MHz): δ 5.35 (18H, $\nu_{1/2}$ = 100 Hz), 4.99 (3H, $\nu_{1/2}$ = 25 Hz), 4.08 (6H, $\nu_{1/2}$ = 30 Hz), -2.42 (6H, $\nu_{1/2}$ = 100 Hz), -6.68 (18H, $\nu_{1/2}$ = 70 Hz), -14.514 (18H, $\nu_{1/2}$ = 200 Hz). Anal. Calcd. for $C_{59}H_{82}BCe$: C, 75.21; H, 8.77. Found C, 74.88; H, 8.67. Full crystallographic details are included as Supporting Information. Monoclinic cell space group $P2_1/n$: a = 10.6158(5) Å, b = 22.808(1) Å, c = 20.588(1) Å, β = 100.579(1) °, V = 4900.3(4) Å^3. The crystal used for structural determination was grown in a C_6D_{12} solution in an NMR tube, and the asymmetric unit contained half a molecule of C_6D_{12}.

NMR tube reaction of CH_3Br or CH_3I and Cp'$_2$CeH in cyclohexane-d$_{12}$.

Cp'$_2$CeH was dissolved in cyclohexane-d$_{12}$ in an NMR tube. The tube was cooled in a liquid nitrogen isopropanol bath, and the head space was evacuated. In the case of

CH_3Br, 1 atm of the gas was added, while in the case of CH_3I, an excess of the liquid was added via vacuum transfer followed by N_2 (1 atm). In both cases, upon warming to 19°C, the solution immediately turned yellow and a yellow precipitate formed. The ^1H NMR spectra contained only resonances due to CH_4 and either Cp'_2CeBr or Cp'_2CeI.

NMR tube reaction of dimethylether and Cp'_2CeH in cyclohexane-d_{12}.

Cp'_2CeH was dissolved in cyclohexane-d_{12} in an NMR tube. The tube was cooled in a liquid nitrogen isopropanol bath, the head space was evacuated and replaced with dimethylether (1 atm). The tube was warmed to 19°C, and the purple solution rapidly turned red. After 15 minutes, resonances due to Cp'_2CeH had disappeared from the ^1H NMR spectrum. Resonances due to Cp'_2CeCH_2OMe and a new pair of paramagnetic resonances [^1H NMR (C_6D_{12}) δ -2.38 (36H, $\nu_{1/2}$ = 15 Hz), -4.43 (18H, $\nu_{1/2}$ = 15 Hz)] had appeared. The ratio of Cp'_2CeCH_2OMe and the unknown species, Q'_{OMe}, was approximately 1.3:1. After two days, resonances due to Cp'_2CeOMe had appeared in the spectrum; the ratio of Cp'_2CeOMe, Cp'_2CeCH_2OMe, and Q'_{OMe} was approximately 1:40:48. The sample was heated at 60°C. After one day, the ratio of the three species was 1:6:5, after 12 days 2.5:2:1, and after 27 days 7:3:1.

NMR tube reaction of trimethylamine and Cp'_2CeH in cyclohexane-d_{12}.

Cp'_2CeH was dissolved in cyclohexane-d_{12}, the sample was cooled in a liquid nitrogen isopropanol bath, the head space was evacuated, and replaced with anhydrous trimethylamine (1 atm). The tube was warmed to 19°C and allowed to stand. After 2 days, the ^1H NMR spectrum contained only paramagnetic resonances due to Cp'_2CeH. The sample was heated at 60°C for 19 days, after which time the ^1H NMR spectrum was unchanged.

NMR tube reaction of CH_3Cl, CH_3Br, or CH_3I and Cp'[$(Me_3C)_2C_5H_2C(Me_2)CH_2$]Ce in cyclohexane-$d_{12}$.

Cp'$_2$Ce($CH_2C_6H_5$) was dissolved in cyclohexane-d_{12} and heated at 60°C for 12 hours, yielding a solution of Cp'[$(Me_3C)_2C_5H_2C(Me_2)CH_2$]Ce. The tube was cooled in a liquid nitrogen isopropanol bath, the head space was evacuated, and replaced with CH_3Cl (1 atm), CH_3Br (1 atm), or an excess of CH_3I via vacuum transfer followed by N_2 (1 atm). The tube was warmed to 19°C and allowed to stand.

In the case of CH_3Cl, after 10 min, the purple solution had turned red. Resonances due to the starting material had disappeared from the ^{1}H NMR spectrum, and a pair of resonances due to Cp'$_2$CeCl[4a] and two new paramagnetic resonances in a 2:1 ratio, Q_{Cl}, had appeared, ^{1}H NMR (C_6D_{12}) -1.36 ($\nu_{1/2}$ = 25 Hz), -8.54 ($\nu_{1/2}$ = 10Hz). The ratio of Q_{Cl} to Cp'$_2$CeCl was 4:1. After 1 hour, the ratio was 1:2, and after 2 hours, the solution was orange and the ratio was 1:5. After 3 days, the solution had turned yellow, yellow crystals had formed, and only resonances due to Cp'$_2$CeCl remained in the spectrum.

In the case of CH_3Br, after 10 min, the purple solution had turned deep orange-brown, and two new paramagnetic resonances in a 2:1 ratio, Q_{Br}, had appeared in the ^{1}H NMR spectrum. After 30 minutes, only the new resonances remained in the spectrum, ^{1}H NMR (C_6D_{12}) -1.36 ($\nu_{1/2}$ = 15Hz), -8.16($\nu_{1/2}$ = 10 Hz). After 7 hours, resonances due to Cp'$_2$CeBr had appeared in the spectrum; the ratio of Q_{Br} to Cp'$_2$CeBr was 1:2, after 3 days, yellow crystals had formed, and only resonances due to Cp'$_2$CeBr remained.

In the case of CH_3I, after 15 min, the purple solution had turned redder, and two new paramagnetic resonances in a 2:1 ratio, Q_I, had appeared in the ^1H NMR spectrum. After 40 minutes, the solution was red-orange, and only the new resonances remained in the spectrum. ^1H NMR (C_6D_{12}) δ -1.29 ($\nu_{1/2}$ = 260 Hz), -7.82 ($\nu_{1/2}$ = 10 Hz). After 3 hours, resonances due to Cp'$_2$CeI had appeared; the ratio of the Q_I to Cp'$_2$CeI was 6:1, after five days, only resonances due to Cp'$_2$CeI remained.

In all cases, GCMS analysis of the hydrolyzate showed one principle component in addition to Cp'H, with $(M)^+$ *m/z* 248 (Cp"H). Resonances due to Cp"Cp'CeCl, Cp"Cp'CeBr, and Cp"Cp'CeI could not be unequivocally assigned; presumably the line widths are broad and the chemical shift differences relative to the resonances of Cp'$_2$CeCl, Cp'$_2$CeBr, and Cp'$_2$CeI are small, unlike in the case of Cp"Cp'CeF where the line widths are narrow.[4a] The hydrolysis experiments provided unequivocal evidence for the presence of Cp"H.

NMR tube reaction of dimethylether and Cp'[$(Me_3C)_2C_5H_2C(Me_2)CH_2$]Ce in cyclohexane-$d_{12}$.

Cp'$_2$Ce($CH_2C_6H_5$) was dissolved in cyclohexane-d_{12} and heated at 60°C for 12 hours, yielding a solution of Cp'[$(Me_3C)_2C_5H_2C(Me_2)CH_2$]Ce. The tube was cooled in a liquid nitrogen isopropanol bath, the head space was evacuated, and replaced with dimethylether (1 atm). The tube was warmed to 19°C, and the deep purple solution rapidly turned red. After 20 minutes, the only paramagnetic resonances in the ^1H NMR spectrum were those of Cp'$_2$CeCH$_2$OMe. The sample was taken to dryness, and the red solid was dissolved in cyclohexane-d_{12}. No new paramagnetic resonances appeared in the ^1H NMR spectrum. The sample was heated at 60°C, and after one day, resonances due to Cp'[$(Me_3C)_2C_5H_2C(Me_2)CH_2$]Ce had appeared in the ^1H NMR

spectrum; the ratio of Cp'_2CeCH_2OMe to $Cp'[(Me_3C)_2C_5H_2C(Me_2)CH_2]Ce$ was approximately 11:1. After three days, the ratio was unchanged. The tube was cooled in a liquid nitrogen isopropanol bath, the head space was evacuated, and the sample was warmed to 19°C. This freeze-pump-thaw procedure was performed two more times, and the headspace was refilled with N_2 (1 atm). The sample was heated for three days at 60°C. The ratio of Cp'_2CeCH_2OMe to $Cp'[(Me_3C)_2C_5H_2C(Me_2)CH_2]Ce$ in the ^1H NMR spectrum remained approximately 11:1.

NMR tube reaction of trimethylamine and $Cp'[(Me_3C)_2C_5H_2C(Me_2)CH_2]Ce$ in cyclohexane-d_{12}.

$Cp'_2Ce(CH_2C_6H_5)$ was dissolved in cyclohexane-d_{12} and heated at 60°C for 12 hours, yielding a solution of $Cp'[(Me_3C)_2C_5H_2C(Me_2)CH_2]Ce$. The tube was cooled in a liquid nitrogen isopropanol bath, the head space was evacuated, and replaced with anhydrous trimethylamine (1 atm). The tube was warmed to 19°C and allowed to stand. After 1 hour, the ^1H NMR spectrum contained three new Me_3C- resonances in a 1:1:1 ratio, ^1H NMR (C_6D_{12}) 6.43 (18H, $\nu_{1/2}$ = 90 Hz), -2.47 (18H, $\nu_{1/2}$ = 40 Hz), -13.60 (18H, $\nu_{1/2}$ = 40 Hz), Q_{NMe2}; resonances due to the CH_2NMe_2 ligand were not observed. The ratio of the new species to $Cp'[(Me_3C)_2C_5H_2C(Me_2)CH_2]Ce$ was 1:1.3. After 3.5 hours, the ratio was 3:1, and after one day, it was 6:1. The sample was heated at 60°C for 2 days, and the ratio was 1.3:1; the ratios did not change upon heating the sample for an additional 15 days.

NMR tube reaction of dimethylether or trimethylamine and $(Cp'-d_{27})\{[C(CD_3)_3]_2C_5H_2[C(CD_3)_2CD_2]\}Ce$ in cyclohexane-d_{12}.

$Cp'_2Ce(CH_2Ph)$ was dissolved in C_6D_6 and heated at 60°C for 4 days to perdeuterate the ring t-butyl groups. The sample was taken to dryness and the solid residue was

redissolved in fresh C_6D_6. The sample was heated for an additional 7 days, then taken to dryness and the solid residue was redissolved in C_6D_{12}. The sample was heated at 60°C for 1 day, yielding a solution of (Cp'-d_{27}){[$C(CD_3)_3$]$_2$$C_5H_2$[$C(CD_3)_2CD_2$]}Ce. The tube was cooled in a liquid nitrogen isopropanol bath, the head space was evacuated, and replaced with dimethylether or trimethylamine (1 atm).

In the case of dimethylether, the tube was warmed to 19°C, and the deep purple solution rapidly turned red. After 30 minutes, the only paramagnetic resonances in the ^{1}H NMR spectrum were those of the Cp'-ring C-H and the OMe group of (Cp'-d_{27})$_2$$CeCH_2OMe$. The ^{2}H NMR spectrum contained resonances due to the Cp'-ring *t*-butyl groups of (Cp'-d_{27})$_2$$CeCH_2OMe$. The ^{13}C NMR spectrum contained a single resonance corresponding to dimethylether. After two days, the spectra were unchanged. The sample was heated at 60°C. After three days, a 1:1:1 pattern (3.16 ppm, J_{HD} = 1.2 Hz) had appeared in the ^{1}H NMR spectrum just upfield of the signal for dimethylether (3.18 ppm). Resonances due to the Cp'-ring *t*-butyl groups of (Cp'-d_{27-x})$_2$$CeCH_2OMe$ had also appeared in the ^{1}H NMR spectrum; the ratio of the integrated intensities of the *t*-butyl resonances at -1.11 and -10.90 ppm was 1:7. The ratio of the corresponding peaks in the ^{2}H NMR spectrum was 3:1, and a broadened triplet (3.20 ppm, J_{HD} = 1.5 Hz) corresponding to partially deuterated dimethylether had also appeared. The ratio of the resonance at -10.90 ppm to the dimethylether resonance was 1:1. In the ^{13}C NMR spectrum, a 1:1:1 pattern (59.95 ppm, J_{CD} = 21 Hz) had appeared just upfield of the signal for dimethylether (60.25 ppm). After seven days, the ratio of the integrated intensities of the resonances at -1.11 and -10.90 ppm in the ^{1}H NMR and ^{2}H NMR spectra were virtually unchanged, but the ratio of the resonance at -10.90 ppm to the dimethylether resonance in the ^{2}H NMR spectrum was 1:4. After 18 days, the ratio of the resonances at -1.11 and -10.90 ppm was 1:2.5

in the ^{1}H NMR spectrum and 12:1 in the ^{2}H NMR spectrum, and the ratio of the resonance at -10.90 ppm to the dimethylether resonance in the ^{2}H NMR spectrum was 1:13. After 81 days, the ratio of the resonances at -1.11 and -10.90 ppm was 1:1 in the ^{1}H NMR spectrum and 2:1 in the ^{2}H NMR spectrum, and the ratio of the resonance at -10.90 ppm to the dimethylether resonance in the ^{2}H NMR spectrum was 1:14.

In the case of trimethylamine, the sample was heated at 60°C. After one day, resonances due to partially protiated (Cp'-d_{27}){[$C(CD_3)_3$]$_2$$C_5H_2$[$C(CD_3)_2CD_2$]}Ce and Q_{NMe2} had appeared in both the ^{1}H and ^{2}H NMR spectra. In addition, a triplet (2.12 ppm, 2 Hz) corresponding to NMe_3-d_1 had appeared in the ^{2}H NMR spectrum. The sample was heated at 60°C for 33 days. The intensity of the paramagnetic resonances in the ^{1}H NMR spectrum had increased substantially, and the corresponding resonances in the ^{2}H NMR spectrum had diminished. A broad resonance presumably corresponding to partially deuterated trimethylamine (2.08 ppm, $\nu_{1/2}$ = 46 Hz) had appeared just upfield of the resonance of trimethylamine (2.10 ppm). The signal was too broadened to discern HD coupling. The multiplet corresponding to partially deuterated trimethylamine in the ^{2}H NMR spectrum had increased in intensity and complexity. The ^{13}C NMR spectrum included a resonance for trimethylamine (46.90 ppm) and a 1:1:1 pattern slightly upfield corresponding to partially deuterated trimethylamine (46.59 ppm, J_{CD} = 20 Hz).

NMR tube reaction of D_2 and Cp'$_2$$CeCH_2OMe$ in cyclohexane-d_{12}.

Cp'$_2$$CeCH_2OMe$ was dissolved in cyclohexane-d_{12} in an NMR tube. The tube was cooled in a liquid nitrogen isopropanol bath, the head space was evacuated, and replaced with D_2 (1 atm). The tube was warmed to 19°C and allowed to stand. After

15 minutes, resonances due to Cp'_2CeOMe and Cp'_2CeD had appeared in the ^1H NMR spectrum. The ^2H NMR spectrum contained resonances due to CH_2DOCH_3. The ratio of Cp'_2CeOMe, Cp'_2CeCH_2OMe, and Cp'_2CeD in the ^1H NMR spectrum was approximately 1:7:8. After two days, the ratio was approximately 1:1:7. After 9 days, resonances due to Cp'_2CeCH_2OMe had disappeared from the spectrum, and the ratio of Cp'_2CeOMe and Cp'_2CeD was approximately 1:5. No resonances for methane were observed. The ^2H NMR spectrum contained resonances due to CH_2DOCH_3 and deuterium incorporation into the Cp'-ring *t*-butyl groups of Cp'_2CeD.

NMR tube reaction of CH_3Br and Cp'_2CeCH_2OMe in benzene-d_6.

Cp'_2CeCH_2OMe was dissolved in benzene-d_6 in an NMR tube. The tube was cooled in a liquid nitrogen isopropanol bath, the head space was evacuated, and replaced with CH_3Br (1 atm). The red solution was warmed to 19°C and allowed to stand. After one day, resonances due to dimethylether, Cp'_2CeBr, Cp'_2CeOMe, and Q_{Br}, had appeared in the ^1H NMR spectrum; the ratio of Cp'_2CeCH_2OMe, Cp'_2CeBr, Cp'_2CeOMe, and Q_{Br} was 8:8:1:2. After 4 days, the solution had turned yellow, and only resonances due to Cp'_2CeBr and dimethylether remained in the spectrum.

NMR tube reaction of CH_3F and Cp'_2CeCH_2OMe in benzene-d_6.

Cp'_2CeCH_2OMe was dissolved in benzene-d_6 in an NMR tube. The tube was cooled in a liquid nitrogen isopropanol bath, the head space was evacuated, and replaced with CH_3F (1 atm). The red solution was warmed to 19°C and allowed to stand. After one day, resonances due to dimethylether and Cp'_2CeF had appeared in the ^1H NMR spectrum; the ratio of Cp'_2CeCH_2OMe to Cp'_2CeF was approximately 30:1. After 2 days, the ratio was 18:1. The sample was warmed to 60°C, and after one day, the red solution had become more orange, and resonances due to Cp'_2CeOMe had appeared;

the ratio of Cp'_2CeCH_2OMe, Cp'_2CeF, and Cp'_2CeOMe was approximately 6.5:2.5:1. After five days, the ratio was 1:4:2, after nine days, only resonances due to Cp'_2CeF, and Cp'_2CeOMe remained in a 1.5:1 ratio.

NMR tube reaction of BPh_3 and Cp'_2CeCH_2OMe in benzene-d_6.

Cp'_2CeCH_2OMe was dissolved in C_6D_6 in an NMR tube and less than an equimolar amount of BPh_3 was added. After 10 minutes, the only paramagnetic resonances in the ^1H NMR spectrum were those due to Cp'_2CeOMe. Integration relative to the solvent residual proton peak indicated that the conversion of Cp'_2CeCH_2OMe to Cp'_2CeOMe was quantitative. The sample was hydrolyzed with basic hydrogen peroxide, and GC MS analysis of the combined organic layers showed that the sample contained a fraction with $(M)^+$ *m/z* 108 ($C_6H_5CH_2OH$) and a smaller fraction with $(M)^+$ *m/z* 122 ($C_6H_5(CH_2)_2OH$) in addition to Cp'H. No fraction corresponding to C_6H_5OH was observed.

NMR tube reaction of BPh_3 and Q_I in benzene-d_6.

$Cp'_2Ce(CH_2C_6H_5)$ was dissolved in cyclohexane-d_{12} and heated at 60°C for 12 hours, yielding a solution of $Cp'[(Me_3C)_2C_5H_2C(Me_2)CH_2]Ce$. The tube was cooled in a liquid nitrogen isopropanol bath, the head space was evacuated, and an excess of CH_3I was added by vacuum transfer. The tube was warmed to 19°C, the headspace was refilled with N_2 (1 atm), and the sample was allowed to stand. After 40 minutes, the solution was red-orange, and only resonances of Q_I remained in the spectrum. A less than an equimolar amount of BPh_3 was added, the sample was agitated and allowed to stand. The resonances due to Q_I disappeared and those of Cp'_2CeI appeared over the course of 1 hour. Integration relative to the solvent residual proton peak indicated that the conversion of Q_I to Cp'_2CeI was quantitative. The sample was

hydrolyzed with basic hydrogen peroxide, and GC MS analysis showed that the sample contained a fraction with $(M)^+$ *m/z* 108 ($C_6H_5CH_2OH$) and a smaller fraction with $(M)^+$ *m/z* 122 ($C_6H_5(CH_2)_2OH$) in addition to Cp'H. No fraction corresponding to C_6H_5OH was observed.

NMR tube reaction of CH_3F and $Cp'_2CeHBPh_3$ in cyclohexane-d_{12}.

Cp'_2CeH was dissolved in cyclohexane-d_{12}, and a slight excess of BPh_3 was added. The purple solution immediately turned yellow, and the ^1H NMR spectrum contained only resonances due to $Cp'_2CeHBPh_3$. The tube was cooled in a liquid nitrogen isopropanol bath, the head space was evacuated, and replaced with CH_3F (1 atm). The sample was warmed to 19°C, and the solution color became slightly more orange. After 10 minutes, the resonances due to free BPh_3 had grown substantially in the ^1H NMR spectrum, and the only significant paramagnetic resonances were those of Cp'_2CeF. Integration relative to the solvent residual proton peak indicated that the conversion of Cp'_2CeH to Cp'_2CeF was approximately 20%.

In a separate experiment, Cp'_2CeF and an excess of BPh_3 were dissolved in benzene-d_6 in an NMR tube. The ^1H NMR spectrum contained only resonances due to the two individual components with no perturbation to their chemical shifts or line shapes. The orange solution was heated at 60°C. After three days, the ^1H NMR spectrum had not changed.

NMR tube reaction of CH_3Br and $Cp'_2CeHBPh_3$ in cyclohexane-d_{12}.

Cp'_2CeH was dissolved in cyclohexane-d_{12}, and a slight excess of BPh_3 was added. The purple solution immediately turned yellow, and the ^1H NMR spectrum contained only resonances due to $Cp'_2CeHBPh_3$. The tube was cooled in a liquid nitrogen

isopropanol bath, the head space was evacuated, and replaced with CH_3Br (1 atm). The sample was warmed to 19°C, and the solution color became more orange. After 10 minutes, the resonances due to free BPh_3 had grown substantially in the ^1H NMR spectrum, and the only significant paramagnetic resonances were those of Cp'_2CeBr. Integration relative to the solvent residual proton peak indicated that the conversion of Cp'_2CeH to Cp'_2CeBr was essentially quantitative. The sample was hydrolyzed with basic hydrogen peroxide, and GC MS analysis of the combined organic layers showed a fraction with $(M)^+$ *m/z* 94 corresponding to C_6H_5OH in addition to Cp'H. No fractions with $(M)^+$ *m/z* 108 ($C_6H_5CH_2OH$) nor $(M)^+$ *m/z* 122 ($C_6H_5(CH_2)_2OH$) were observed.

Computational details

The Stuttgart-Dresden-Bonn Relativistic large Effective Core Potential (RECP)[36a] was used to represent the inner shells of Ce. The associated basis set[36a] augmented by an f polarization function (α = 1.000) was used to represent the valence orbitals.[36b] F was also represented by an RECP[37a] with the associated basis set of the type (4s5p/2s3p)[37a] augmented by two contracted d polarisation gaussian functions (α_1 = 3.3505(0.357851), α_2 = 0.9924(0.795561)).[37b] The atoms Cl, Br, and I were represented by an RECP[37c] with the associated basis set of the type (4s5p/2s3p)[37c] augmented by a single d polarization gaussian function with exponent of 0.643, 0.550 and 0.730 respectively.[37b] The atoms C, O, and H were represented by an all-electron 6-31G(d, p) basis set.[38] Calculations were carried out at the DFT(B3PW91) level[39] with Gaussian 03.[40] The nature of the extrema (minimum or transition state) was established with analytical frequencies calculations and the intrinsic reaction coordinate (IRC) was followed to confirm that the transition states connect to

reactants and products. The zero point energy (ZPE) and entropic contribution have been estimated within the harmonic potential approximation. The Gibbs free energy, G, was calculated at T = 298.15K. Using gas phase calculations for evaluating the entropic contribution to reactions in solution is an approximation; in particular, the translational degrees of freedom are exaggerated.[41] However, the trends are properly calculated especially for a similar set of molecules as is the case here. This is supported by the observation that using E in place of G gives similar profiles and similar ranking as a function of X as shown in the Supporting Information. Thus, the trends in G are reliable even though the absolute values are not. The NBO analysis[42] was carried out replacing Ce by La because of the technical requirement to have an even number of f electrons for the calculations; these values are included in the Supporting Information for the inquisitive reader. Since the solvent used in the experimental studies was a hydrocarbon, such as cyclohexane or benzene, no large solvent effect on the reactants and products is expected. Consequently, no solvation effects were introduced in the computational studies.

Acknowledgment

This work was supported by the Director, Office of Science, Office of Basic Energy Sciences (OBES), of the U.S. Department of Energy (DOE) under Contract No. DE-AC02-05CH11231. We thank F. J. Hollander at CHEXRAY, the U.C. Berkeley X-ray diffraction facility, for help with the crystallography. L.M thanks the CINES and CALMIP for a generous grant of computing time. L.M. is also member of the Institut Universitaire de France, L.M. and O.E thank the CNRS and Ministère de l'Enseignement Supérieur et de la Recherche for funding, and A.Y. thanks the CEA for PhD fellowship.

Supporting information

Additional experimental details, X-ray crystallographic data (CIF), CCD numbers, Coordinates and potential energies, E, and Gibbs free energies, G, values in a.u. for all calculated structures. Energy profiles for the reactions shown in Figure 5 using energies E. Table of NBO charges. This material is available free of charge via the Internet at http:// pubs.acs.org. Crystallographic data for the structures in this paper have also been deposited with the Cambridge Crystallographic Data Center. Copies of the data CCDC 711256 for $[1,2,4\text{-}(Me_3C)_3C_5H_2]_2CeCH_2OMe$, and CCDC 711255 for $[1,2,4\text{-}(Me_3C)_3C_5H_2]_2Ce(H)(BPh_3)$ can be obtained free of charge via www. ccdc.cam.ac.uk/data_request/cif, by e-mailing data_request@ccdc.cam.ac.uk, or by contacting The Cambridge Crystallographic Data Center, 12 Union Road, Cambridge CB2 1EZ, UK; fax +44 1223 336033.

References

1) Werkema, E. L.; Messines, E.; Perrin, L.; Maron, L.; Eisenstein, O.; Andersen, R. A. *J. Am. Chem. Soc.* **2005**, *127*, 7781.

2) Slayden, S. W.; Liebman, J. F.; Mallard; W. G. in " The Chemistry of Halides, Pseudohalides and Azides" Supp D2, Patai, S. and Rappoport, Z. Eds. Wiley, Chichester 1995, pp 386.

3) Pankratz, L. B. "Thermodynamic Properties of Halides, Bulletin 674, Bureau of Mines", 1984.

4) (a) Werkema, E. L.; Maron, L.; Eisenstein, O.; Andersen, R. A. *J. Am. Chem. Soc.* **2007**, *129*, 2529. (b) Werkema, E. L.; Maron, L.; Eisenstein, O.; Andersen, R. A. *J. Am. Chem. Soc.* **2007**, *129*, 6662.

5) Maron, L.; Werkema, E.; Perrin, L.; Eisenstein, O.; Andersen, R. A. *J. Am. Chem. Soc.* **2005**, *127*, 279.

6) Zi, G.; Blosch, L. L.; Jia, L.; Andersen, R. A. *Organometallics* **2005**, *24*, 4602.

7) Werkema, E.; Andersen, R. A. *J. Am. Chem. Soc.* **2008**, *130*, 7153.

8) Heeres, H. J.; Renkema, J.; Booij, M.; Meetsma, A.; Teuben, J. *Organometallics* **1988**, *7*, 2495.

9) Booij, M.; Meetsma, A.; Teuben, J. H. *Organometallics* **1991**, *10*, 3246.

10) Ph. D. Thesis of Werkema, E. L. University of California, Berkeley, 2005.

11) Heeres, H. J.; Meetsma, A.; Teuben, J. H.; Rogers, R. D. *Organometallics*, **1989**, *8*, 2637.

12) Allen, F. H.; Kennard, O.; Watson, D. G.; Brammer, L.; Orpen, G. A.; Taylor, R. *J. Chem. Soc., Perkin Trans,* **1987**, *2*, S1.

13) (a) Clark, T.; Schleyer, P. v. R.; Houk, K. N.; Rondan, N. G. *J. Chem. Soc., Chem. Commun.* **1981**, 579. (b) Boche, G.; Opel, A.; Marsch, M.; Harms, K.; Haller, F.; Lorenz, J. C. W.; Thummler, C.; Koch, W. *Chem. Ber.-Rec.* **1992**, *125*, 2265. (c) Boche, G.; Lohrenz, J. C. *Chem. Rev.* **2001**, *101*, 697. Braun, W. in Patai Series, The Chemistry of Organolithium Compounds, Part 2. Rappoport, Z.; Marek, I. Eds. 2008. Chap. 13. Wiley, New York, NY.

14) Erker, G.; Schlund, P.; Krüger, C. *J. Chem. Soc. Chem. Commun.* **1986**, 1403.
The two distances are inverted compared to the distances in $Cp'_2Ce(\eta^2\text{-}CH_2OMe)$ and expectation. However, all of the heavy atoms in the crystal structure of the zirconium compound are refined isotropically in the CCDC, resulting in considerable uncertainty

in the distances. The calculated structure of $Cp_2Zr(\eta^2\text{-}CH_2OMe)$ yields Zr-CH_2 = 2.249 Å, CH_2-O = 1.444 Å, Zr-O = 2.328 Å, which differ somewhat from the corresponding experimental values of 2.271(5), 1.414(6) and 2.204(3) Å, however, the oxygen is pyramidal as found in the X-ray crystal structure. The calculated distances are therefore in accord with the experimental values for $Cp'_2Ce((\eta^2\text{-}CH_2OMe)$.

15) Buchwald, S. L.; Nielsen, R. B.; Dewan, J. C. *Organometallics* **1989**, *8*, 1593.

16) Lork, E.; Gortier, B.; Knapp, C.; Mews, R. *Solid State Sci*. **2002**, *4*, 1403.

17) (a) Meerwein, H.; Burneleit, W. *Ber. Dtsch. Chem. Ges*. **1928**, *61*, 1840. (b) Meerwein, H. *Angew. Chem*. **1948**, *60*, 78.

18) Bawn, C. E. H.; Ledwith, A. *Prog. Boron Chem*. **1964**, *1*, 345.

19) Leffler, J. E.; Ramsey, B. G. *Proc. Chem. Soc*. **1961**, 117.

20) Köster, R.; Rickborn, B. *J. Am. Chem. Soc*. **1967**, *89*, 2782.

21) (a) Musker, W. K.; Stevens, R. R. *Inorg. Chem*. **1969**, *8*, 255. (b) Bickelhaupt, F.; Barnick, J. W. F. K. *Rec. Trav. Chim*. **1968**, *87*, 188.

22) Stoddard, J. M.; Shea, K. J. *Organometallics* **2003**, *22*, 1124.

23) (a) Piers, W. E. *Adv. Organomet. Chem*. **2005**, *52*, 1. (b) Erker, G. *Dalton Trans*. **2005**, 1883.

24) Choukroun, R.; Lorber, C.; Vendier, L.; Lepetit, C. *Organometallics* **2006**, *25*, 1551.

25) Choukroun, R.; Lorber, C.; Donnadieu, B. *Organometallics* **2004**, *23*, 1434.

26) Yang, X.; Stern, C. L.; Marks, T. J. *Angew Chem. Int. Ed. Engl.* **1992**, *31*, 1375.

27) Bau, R.; Teller, R. G.; Kirtley, S. W.; Koetzle, T. F. *Acc. Chem. Res.* **1979**, *12*, 176.

28) (a) Lias, S. G.; Bartmess, J. E.; Liebman, J. F.; Holmes, J. L.; Levin, R. D.; Mallard, W. G. *J. Phys. Chem. Ref. Data* **1988**, *17*, 647. (b) Dewar, M. J. S.; Dieter, K. M. J. *J. Am. Chem. Soc.* **1986**, *108*, 8075.

29 (a) Closs, G. L.; Closs, L. E. *Angew. Chem.* **1962**, *74*, 431. (b) Closs, G. L.; Closs, L. E. *J. Am. Chem. Soc.* **1963**, *85*, 99.

30) Bauschlicher, C. W.; Haber, K.; Schaefer, H. F. III, Bender, C. F. *J. Am. Chem. Soc.* **1977**, *99*, 3610.

31) Clark, T.; Schleyer, P. v. R.; Houk, K. N.; Rondan, N. G. *J. Chem. Soc., Chem. Commun.* **1981**, 579. Boche, G.; Opel, A.; Marsch M.; Harms, K.; Haller, F.; Lohrenz, J. C. W.; Thümmler, C.; Koch, W. *Chem. Ber.*, **1992**, *125*, 2265. Hermann, H.; Lohrenz, J. C.; Kühn, A.; Boche, G. *Tetrahedron* **2000**, *56*, 4109. Naruse, Y.; Hayashi, A.; Sou, S.-i.; Ikeda, H.; Inagaki, S. *Bull Chem Soc. Jpn.* **2001**, *74*, 245. Pratt, M.; Ramachandran, B.; Xidos, J. D.; Cramer, C. J.; Truhlar, D. G. *J. Org. Chem.* **2002**, *67*, 7607.

32) Nolan, S. P.; Stern, D.; Marks, T. J. *J. Am. Chem. Soc.* **1989**, *111*, 7844. The values for X = OMe and NMe_2 are given in this article and the values for X = Cl, Br, and I are determined using BDE values in (a) McMillen, D. F.; Golden, D. M. *Ann Rev. Phys. Chem.* **1982**, *33*, 493. (b) Blanksby, S. J.; Ellison, G. B. *Acc. Chem. Res.* **2003**, *36*, 255.

33) (a) Weinhold, F.; Landis, C. *Valency and Bonding: a natural bond orbital donor Acceptor Perspective*. Cambridge University Press, Cambridge, UK, 2005. p 138. (b) Bent H. A. *Chem. Rev*. **1961**, *61*, 275.

34) Sofield, C. D.; Andersen, R. A. *J. Organomet. Chem* **1995**, *501*, 271.

35) Weber, F.; Sitzmann, H.; Schultz, M.; Sofield, C. D.; Andersen, R. A. *Organometallics* **2002**, *21*, 3139.

36) (a) Dolg, M.; Stoll, H.; Savin, A.; Preuß, H. *Theor. Chim. Acta* **1989**, *75*, 173. Dolg, M.; Stoll, H.; Preuß, H. *Theor. Chim. Acta* **1993**, *85*, 441. (b) Maron, L. Eisenstein, O. *J. Phys. Chem. A*, **2000**, *104*, 7140.

37) (a) Igel-Mann, H.; Stoll, H.; Preuß, H. *Mol. Phys*. **1988**, *65*, 1321. (b) Maron, L.; Teichteil, C. *Chem. Phys*. **1998**, *237*, 105. (c) Bergner, A.; Dolg, M. ; Küchle, W.; Stoll, H.; Preuß, H. *Mol. Phys*. **1993,** *80*, 1431.

38) Hariharan, P. C.; Pople, J. A. *Theor. Chim. Acta* **1973**, *28*, 213.

39) Perdew, J. J. P.; Wang, Y. *Phys. Rev. B*, 1992, **82**, 284. Becke, A. D. *J. Chem. Phys*. **1993**, *98*, 5648. Burke, K.; Perdew, J. P.; Yang, W. in "*Electronic Density Functional Theory: Recent Progress and New Directions"* Dobson, J. F.; Vignale, G., Das, M. P. Eds. **1998**, Plenum.

40) Gaussian 03, Revision C.02, Frisch, M. J.; Trucks, G. W.; Schlegel, H. B.; Scuseria, G. E.; Robb, M. A.; Cheeseman, J. R.; Montgomery, Jr., J. A.; Vreven, T.; Kudin, K. N.; Burant, J. C.; Millam, J. M.; Iyengar, S. S.; Tomasi, J.; Barone, V.; Mennucci, B.; Cossi, M.; Scalmani, G.; Rega, N.; Petersson, G. A.; Nakatsuji, H.; Hada, M.; Ehara, M.; Toyota, K.; Fukuda, R.; Hasegawa, J.; Ishida, M.; Nakajima, T.; Honda, Y.; Kitao, O.; Nakai, H.; Klene, M.; Li, X.; Knox, J. E.; Hratchian, H. P.;

Cross, J. B.; Bakken, V.; Adamo, C.; Jaramillo, J.; Gomperts, R.; Stratmann, R. E.; Yazyev, O.; Austin, A. J.; Cammi, R.; Pomelli, C.; Ochterski, J. W.; Ayala, P. Y.; Morokuma, K.; Voth, G. A.; Salvador, P.; Dannenberg, J. J.; Zakrzewski, V. G.; Dapprich, S.; Daniels, A. D.; Strain, M. C.; Farkas, O.; Malick, D. K.; Rabuck, A. D.; Raghavachari, K.; Foresman, J. B.; Ortiz, J. V.; Cui, Q.; Baboul, A. G.; Clifford, S.; Cioslowski, J.; Stefanov, B. B.; Liu, G.; Liashenko, A.; Piskorz, P.; Komaromi, I.; Martin, R. L.; Fox, D. J.; Keith, T.; Al-Laham, M. A.; Peng, C. Y.; Nanayakkara, A.; Challacombe, M.; Gill, P. M. W.; Johnson, B.; Chen, W.; Wong, M. W.; Gonzalez, C.; Pople, J. A.; Gaussian, Inc., Wallingford CT, 2004.

(41) Leung, B. O. ; Reid, D. L. ; Armstrong, D. A. ; Rauk, A. *J. Phys. Chem. A* **2004**, *108*, 2720.

42) Reed, A. E.; Curtiss, L. A.; Weinhold, F. *Chem. Rev*. **1988**, *88*, 899.

TOC

A one-step or two-step pathway for the H for X exchange reactions: that is the question.